Internet Appendix:

Forward Return Expectations*

Mihir Gandhi, Niels Joachim Gormsen, and Eben Lazarus

November 2025

Contents

*Contact: mihir.a.gandhi@gmail.com; niels.gormsen@chicagobooth.edu; lazarus@berkeley.edu.

A Proofs

Proof of Proposition 1. Given that $M_{t,t+n}R_{t,t+n} = 1$ by assumption, $\mathcal{C}_t^{(n)} = 0$ in (4). The stated results then follow immediately. □

Proof of Proposition 2. First consider $n = m = 1$, and write

$$\begin{aligned}\varepsilon_{t+1}^{(1)} = \mu_{t+1}^{(1)} - f_t^{(1)} = \mathscr{L}_{t+1}^{(1)} - \mathscr{L}_t^{(2)} + \mathscr{L}_t^{(1)} + \operatorname{cov}_t(MR_{t,t+2}, r_{t,t+2}) \\ - \operatorname{cov}_t(MR_{t,t+1}, r_{t,t+1}) - \operatorname{cov}_{t+1}(MR_{t+1,t+2}, r_{t+1,t+2}).\end{aligned} \tag{A1}$$

Consider the first covariance term. Given the joint log-normality of the SDF and returns (and the normality of $r_{t,t+n}$), Stein's lemma gives that

$$\begin{aligned}\operatorname{cov}_t(MR_{t,t+2}, r_{t,t+2}) &= \operatorname{cov}_t(MR_{t,t+1}MR_{t+1,t+2}, r_{t,t+2}) \\ &= \operatorname{cov}_t(mr_{t,t+1} + mr_{t+1,t+2}, r_{t,t+2})\,\mathbb{E}_t[MR_{t,t+2}] \\ &= \operatorname{cov}_t(mr_{t,t+1} + mr_{t+1,t+2}, r_{t,t+1} + r_{t+1,t+2})\,,\end{aligned}$$

where $mr_{t,t+n} = \ln(MR_{t,t+n})$, and where the last line uses that $\mathbb{E}_t[MR_{t,t+2}] = 1$. Having separated the two MR terms, apply Stein's lemma again to obtain

$$\begin{aligned}\operatorname{cov}_t(MR_{t,t+2}, r_{t,t+2}) &= \operatorname{cov}_t(mr_{t,t+2}, r_{t,t+1}) + \operatorname{cov}_t(mr_{t,t+1}, r_{t+1,t+2}) + \operatorname{cov}_t(mr_{t+1,t+2}, r_{t,t+2}) \\ &= \operatorname{cov}_t(MR_{t,t+2}, r_{t,t+1}) + \operatorname{cov}_t(MR_{t,t+1}, r_{t+1,t+2}) \\ &\quad + \operatorname{cov}_t(MR_{t+1,t+2}, r_{t+1,t+2})\,.\end{aligned} \tag{A2}$$

For the first two terms in (A2), by the law of total covariance and using that $\mathbb{E}_{t+1}[MR_{t+1,t+2}] = 1$,

$$\begin{aligned}\operatorname{cov}_t(MR_{t,t+2}, r_{t,t+1}) &= \mathbb{E}_t\big[MR_{t,t+1}r_{t,t+1}\operatorname{cov}_{t+1}(MR_{t+1,t+2}, 1)\big] \\ &\quad + \operatorname{cov}_t(MR_{t,t+1}\,\mathbb{E}_{t+1}[MR_{t+1,t+2}], r_{t,t+1}) \\ &= \operatorname{cov}_t(MR_{t,t+1}, r_{t,t+1})\,,\end{aligned} \tag{A3}$$

$$\begin{aligned}\operatorname{cov}_t(MR_{t,t+1}, r_{t+1,t+2}) &= \mathbb{E}_t[MR_{t,t+1}\operatorname{cov}_{t+1}(1, r_{t+1,t+2})] + \operatorname{cov}_t(MR_{t,t+1}, \mathbb{E}_{t+1}[r_{t+1,t+2}]) \\ &= \operatorname{cov}_t(MR_{t,t+1}, \mathbb{E}_{t+1}[r_{t+1,t+2}])\,.\end{aligned} \tag{A4}$$

Turning now to the last term in (A1), the law of total covariance can similarly be applied to obtain that as of time t,

$$\mathbb{E}_t[\operatorname{cov}_{t+1}(MR_{t+1,t+2}, r_{t+1,t+2})] = \operatorname{cov}_t(MR_{t+1,t+2}, r_{t+1,t+2}). \tag{A5}$$

Taking expectations in (A1), substituting in results (A2)–(A5), and applying the definition of $\widehat{\varepsilon}_{t+1}^{(1)}$, we obtain:

$$\mathbb{E}_t\left[\varepsilon_{t+1}^{(1)}\right] = \mathbb{E}_t\left[\widehat{\varepsilon}_{t+1}^{(1)}\right] + \operatorname{cov}_t(MR_{t,t+1}, \mathbb{E}_{t+1}[r_{t+1,t+2}])\,. \tag{A6}$$

Rearranging to solve for $\mathbb{E}_t[\widehat{\varepsilon}_{t+1}^{(1)}]$ yields the stated result for the $n = m = 1$ case. While this case is convenient for straightforward derivations, note that all the above steps apply when using $t + n$ in place of $t + 1$ and using $t + n + m$ in place of $t + 2$, so the stated result holds for general n, m. □

Proof of Proposition 3. Starting again with (A1) and expanding the first covariance term,

$$\operatorname{cov}_t(MR_{t,t+2}, r_{t,t+2}) = \operatorname{cov}_t(MR_{t,t+1}MR_{t+1,t+2}, r_{t,t+1}) + \operatorname{cov}_t(MR_{t,t+1}MR_{t+1,t+2}, r_{t+1,t+2}). \quad \text{(A7)}$$

We consider each of the two terms on the right side of (A7) in turn, and in both cases apply the law of total covariance. For the first term, as in (A3),

$$\operatorname{cov}_t(MR_{t,t+1}MR_{t+1,t+2}, r_{t,t+1}) = \operatorname{cov}_t(MR_{t,t+1}, r_{t,t+1})\,. \quad \text{(A8)}$$

For the second term,

$$\begin{aligned}\operatorname{cov}_t(MR_{t,t+1}MR_{t+1,t+2}, r_{t,t+2}) = \mathbb{E}_t\big[MR_{t,t+1}\operatorname{cov}_{t+1}(MR_{t+1,t+2}, r_{t+1,t+2})\big] \\ + \operatorname{cov}_t(MR_{t,t+1}, \mathbb{E}_{t+1}[r_{t+1,t+2}])\,. \quad \text{(A9)}\end{aligned}$$

Using (A8) and (A9) in (A1), applying the definition of $\widehat{\varepsilon}^{(1)}_{t+1}$, and taking expectations,

$$\begin{aligned}\mathbb{E}_t\left[\varepsilon^{(1)}_{t+1}\right] &= \mathbb{E}_t\left[\widehat{\varepsilon}^{(1)}_{t+1}\right] + \mathbb{E}_t[(MR_{t,t+1}-1)\operatorname{cov}_{t+1}(MR_{t+1,t+2}, r_{t+1,t+2})] \\ &\quad + \operatorname{cov}_t(MR_{t,t+1}, \mathbb{E}_{t+1}[r_{t+1,t+2}]) \\ &= \mathbb{E}_t\left[\widehat{\varepsilon}^{(1)}_{t+1}\right] + \operatorname{cov}_t(MR_{t,t+1}, \mathbb{E}_{t+1}[r_{t+1,t+2}] + \operatorname{cov}_{t+1}(MR_{t+1,t+2}, r_{t+1,t+2}))\,. \quad \text{(A10)}\end{aligned}$$

Note from (4) that $\mathscr{L}^{(1)}_{t+1} = \mathbb{E}_{t+1}[r_{t+1,t+2}] + \operatorname{cov}_{t+1}(MR_{t+1,t+2}, r_{t+1,t+2})$. Using this in (A10),

$$\mathbb{E}_t\left[\widehat{\varepsilon}^{(1)}_{t+1}\right] = \mathbb{E}_t\left[\varepsilon^{(1)}_{t+1}\right] - \operatorname{cov}_t\left(MR_{t,t+1}, \mathscr{L}^{(1)}_{t+1}\right).$$

The above steps again apply when using $t+n$ in place of $t+1$ and using $t+n+m$ in place of $t+2$, completing the proof. □

Proof of Lemma A1. To compute the risk-neutral expectation of $g(P_T) = R^\alpha (\ln R)^\beta$, we apply the Carr and Madan (1998) formula. Under standard regularity conditions, we have

$$\begin{aligned}\frac{1}{R_f}\,\mathbb{E}^*_t\left[R^\alpha (\ln R)^\beta\right] &= \left[g(\bar{P}) - \bar{P}g'(\bar{P})\right]\frac{1}{R_f} + g'(\bar{P})\,P_t \\ &\quad + \int_0^{\bar{P}} g''(K)\,\text{put}(K)dK + \int_{\bar{P}}^{\infty} g''(K)\,\text{call}(K)dK,\end{aligned}$$

where $g'(P) \equiv \frac{\partial g}{\partial P}$ and $g''(P_T) \equiv \frac{\partial^2 g}{\partial P^2}$. The result follows by setting $\bar{P} = F^{(n)}_t$ and simplifying. □

Proof of Proposition A1. (A14) is immediate from Martin (2017) Result 8. (A15) and (A16) follow from Lemma A1 by setting the appropriate α and β and simplifying. □

B Measurement Details

B.1 Options Data

U.S. Data. For the 1996 to 2021 period, we obtain end-of-day option prices, index prices, projected dividend yields, and risk-free rates from OptionMetrics. To maximize the sample size, we use options with non-standard expirations (weekly) and settlement (PM). We use the bid/ask midpoint as the option price in the main analysis. We linearly interpolate the risk-free rate curve to match option

maturities. If either the dividend yield or risk-free rate is missing, we use the last non-missing observation.

For the 1990 to 1995 period, we obtain intraday option prices from CBOE Market Data Replay, as in Culp, Nozawa, and Veronesi (2018). We obtain end-of-day index prices/returns from CRSP and estimate dividend yields from lagged one-year cum/ex-dividend index returns. We obtain Treasury bill rates and constant maturity Treasury yields from FRED to construct risk-free rates, again following Culp, Nozawa, and Veronesi.[1]

Unlike OptionMetrics, CBOE provides intraday quotes. To construct end-of-day prices, we first apply filters to the intraday data and then use the last available quote. We drop quotes with the missing codes of 998 or 999. We drop quotes with negative bid-ask spreads. We correct erroneously recorded quotes — quotes with strike price less than 100 — by multiplying the strike/option price by 10. We drop end-of-day quotes that increase and then decrease fourfold (or vice versa), following similar filters in Andersen, Bondarenko, and Gonzalez-Perez (2015) and Duarte, Jones, and Wang (2024). We interpret these large reversals as probable data errors. To validate these filters, we compare data from CBOE and OptionMetrics in 1996. We match approximately 99.3% of option prices in OptionMetrics, suggesting these filters are not unreasonable.

We apply standard filters to the end-of-day data, as in Constantinides, Jackwerth, and Savov (2013), among others. (1) We drop options with special settlement. (2) To eliminate duplicate quotes, we select the quote with highest open interest. (3) We drop options with fewer than seven days-to-maturity. (4) We drop options with price less than 0.01. (5) We drop options with zero bid prices or negative bid-ask spreads. (6) We drop options that violate static no-arbitrage bounds:

$$\text{put}(K) \leq Ke^{-r\tau} \qquad \text{call}(K) \leq P_t.$$

(7) We drop options for which the Black-Scholes implied volatility computation does not converge and options with implied volatility less than 5% or greater than 100%.

Global Data. We again obtain end-of-day option prices, index prices, projected dividend yields, and risk-free rates from OptionMetrics. Unlike the U.S. data, most option prices are either end-of-day settlement prices or last traded prices. Only a small fraction are from either bid/ask prices. The index price is time synchronized to the option price. If the index price is missing, we obtain the end-of-day price from Compustat Global. Risk-free rates are from currency-matched LIBOR curves. Dividend yields are from put-call parity and so are maturity-specific. As before with risk-free rates, we linearly interpolate the dividend yield curve to match option maturities. We apply the same filters to the end-of-day data as with the U.S. data, except for filters that require bid/ask prices.

Table A1 describes the global sample. The Europe and pan-Europe sample begins in January 2002 and ends in September 2021. The Asia-Pacific sample begins in January 2004 and ends in April 2021. Our global sample closely follows Kelly, Pástor, and Veronesi (2016) and Dew-Becker and Giglio (2023), but we also use pan-European Stoxx indexes. These indexes represent a substantive addition to the sample. At long maturities, the Euro Stoxx 50 is arguably the most liquid options market in the world, as is the case with the dividend futures market.[2]

Main Sample. As the global data is not equally robust across exchanges, we select the most reliable exchanges for the main analysis. We select the main sample by elimination. First, we drop Belgium, Finland, Netherlands, the Stoxx Europe 50/600, Korea, and Taiwan because they do not consistently

[1]The CBOE website is `https://datashop.cboe.com/mdr-quotes-trades-data`.

[2]For more details about the dividend futures market, see Binsbergen and Koijen (2017).

have dense option surfaces, as seen in Panel A of Figure A11. Second, we drop Belgium, Korea, and Taiwan because they do not consistently have long-maturity options, as seen in Figure A12. Finally, we drop Finland, the Stoxx Europe 50/600, Sweden, China, and Japan because they do not consistently have deep out-of-the-money options, as seen in Figure A13. After dropping these exchanges, several for multiple reasons, we have 10 exchanges for the main sample, as seen in the last column of Table A1. As a robustness check, we examine the full sample of 20 exchanges in Table A8.

B.2 Option-Based Implementation

Methodology. On each date and separately for puts/calls,

1. We convert option prices to implied volatilities via Black-Scholes. We follow an extensive literature on option-implied risk-neutral densities that finds interpolation/extrapolation more conducive in the space of implied volatilities, not option prices.[3]

2. We fit a Delaunay triangulation to implied volatilities. The grid consists of strike prices between $\underline{K} = 0.10 \times P_t$ and $\overline{K} = 2.00 \times P_t$ with $\Delta K = 0.001 \times P_t$ and maturities $\tau = 30$, 60, 91, 122, 152, 182, 273, 365 days. The triangulation extrapolates as necessary with the nearest implied volatility in simple moneyness and time-to-maturity space.[4]

3. We convert the triangulation of implied volatilities back to option prices via Black-Scholes. We then use the implied triangulation of option prices to evaluate the LVIX integral in (7) via Gaussian quadrature.

4. With the LVIX in hand, we can compute spot rates, forward rates, and forecast errors via Proposition 1, as visualized in Figure A9.

5. We occasionally find negative forward rates. Gao and Martin (2021) argue that negative forward rates are unlikely theoretically and likely represent data errors. We follow Gao and Martin and drop such observations, but our results are not quantitatively sensitive to this choice.

Discussion. Our methodology addresses the main empirical challenges in moment computation: discretization, truncation, and interpolation bias. Discretization and truncation bias relate to the strike dimension of option prices, interpolation bias to the maturity dimension. Our contribution is not to identify these biases — our discussion below closely follows that in Jiang and Tian (2007), among others — but rather to examine the implications for the LVIX.

First, discretization bias arises because (7) requires numerical integration. To address this bias, we integrate on a fine grid of interpolated option prices in step 3. Second, truncation bias arises because (7) requires integration over an infinite range of strikes in theory. In practice, we truncate the integral. To address this bias, we extrapolate and integrate over strikes well beyond the range of observable options in step 2. Finally, interpolation bias arises because (7) typically requires options with unavailable maturities. For example, we do not typically observe options with exactly 182 or 365 days-to-maturity. To address this bias, we interpolate the volatility surface at target maturities in step 2.

Our main concern is that the bias varies systematically. One possibility is cross-sectional variation: the bias is larger at longer maturities. If we overestimate long-maturity forward rates, then we would

[3]For reviews of the literature on risk-neutral densities, see Figlewski (2010) and Malz (2014).

[4]We implement the Delauney triangulation in Matlab via the `scatteredInterpolant` function.

find more negative forecast errors. Another possibility is business-cycle variation: the bias is larger in bad times. If we overestimate forward rates in bad times, then we would find more predictable forecast errors. In either case, measurement error works against the rational expectations null.

We examine the role of measurement error in Appendix C below.

B.3 CFO Survey Data Break

As discussed in Section 3.2.2, the CFO survey underwent a change in administration in 2020. Prior to 2020, the survey was run by Duke University's Fuqua School of Business (overseen by John Graham and Campbell Harvey). In spring 2020, it was announced that the survey would be run as a collaborative partnership between Duke, the Federal Reserve Bank of Richmond, and the Federal Reserve Bank of Atlanta; see Graham et al. (2020) for details. The redesign affected the sample composition, the survey design, and the way return expectations are elicited.[5]

These changes induce a discrete level shift in forward return expectations, as shown in Figure A4. The top panel of the figure plots the raw (unadjusted) 1-year, 9-year CFO forward risk premium series. The upward shift in 2020 is clearly evident: the post-2020 CFO sample predicts substantially higher returns unconditionally than the previous sample did, and the pre-to-post-2020 shift swamps the cyclical variation in the entire pre-2020 sample. If left uncorrected, this break would affect estimates of CFO forward-rate cyclicality (which estimate covariances between the forward rate and cyclical proxies) and any regressions on CFO forward rates, confounding true cyclical movements with the survey redesign itself.

To correct for this structural break, all of our CFO-based regressions and analyses include an indicator variable that equals one from 2020 onward. The bottom panel of Figure A4 plots the CFO forward risk premia after removing the fitted effect of this post-2020 indicator. Once this level shift is taken out, the series appears much more stable and comparable across the full 2001–2025 sample, and the cyclical patterns we document are not driven mechanically by the survey redesign. The regressions also drop two observations in 2019 that mix forward rates from before the survey redesign (when the survey was run by Duke Fuqua) with realized spot rates from after the survey redesign (when the survey was run by a collaborative partnership).

C Measurement Error in Option-Based Statistics

As introduced in Appendix B.2, our option-based estimation faces the possibility of measurement error. We consider the effect of such measurement error here.

C.1 Alternative Integration Bounds

Theory. We first analyze truncation bias in theory. To motivate the analysis, we note that the integrand in (7) — the option price divided by the strike price — approaches zero in both integration limits:

$$\lim_{K\to 0} \frac{\text{put}(K)}{K} = 0 \qquad \lim_{K\to\infty} \frac{\text{call}(K)}{K} = 0.$$

[5] See the announcement (Graham et al. 2020) for details on the sample composition. For return expectations, the pre-2020 surveys effectively cued respondents to think in terms of excess returns by providing the current Treasury yield on the same screen as the question about S&P return expectations (e.g., see https://cfosurvey.fuqua.duke.edu/wp-content/uploads/2019/12/2019-Q4-US-Toplines-1.pdf); the current surveys no longer provide that information (see https://frbaressurvey.co1.qualtrics.com/jfe/form/SV_23m5JZjAa82BE3j).

This implies that *all* of the integral's mass corresponds to observable, near-the-money strikes and *none* corresponds to unobservable, deep out-of-the-money strikes. Figure A10 visualizes this point in the Black-Scholes model.

Our point above is qualitative: truncation bias might not be large and might even be small. To understand the quantitative implications, we turn to simulations of parametric option pricing models. With knowledge of the true data generating process, we can quantify how methodological choices — truncation of the integral and extrapolation of the implied volatility surface — affect truncation bias. We focus on how the bias varies between short and long maturities as well as good and bad times. Our thought experiment closely follows a similar exercise for the VIX in Jiang and Tian (2007).

Figure A1 reports the results. Panel A truncates the volatility surface. As an example, the 20% truncation bound evaluates the integral from strike $\underline{K} = 0.80 \times P$ to $\overline{K} = 1.20 \times P$. On the left, we consider a Black-Scholes model. We find a small truncation bias in good times but a large truncation bias in bad times. In good times, volatility is low, deep out-of-the-money options are cheap, and so the bias is small. In contrast, in bad times, volatility is high, deep out-of-the-money options are expensive, and so the bias is large. The bias in forward rates is especially large because longer-maturity option prices have more time value. On the right, we consider a stochastic volatility model with jumps (SVJ). We again find an uncomfortably large truncation bias. Relative to Black-Scholes, the bias is larger when volatility is low, but smaller when volatility is high because volatility mean reverts in SVJ.[6]

Panel B extrapolates the volatility surface. As an example, the 20% extrapolation bound first truncates the volatility surface at the 20% out-of-the-money strike, then extrapolates the surface with the corresponding implied volatility, and finally evaluates the integral from strike $\underline{K} = 0.10 \times P$ to $\overline{K} = 2.00 \times P$. We continue with a SVJ model. Relative to Panel A, we find that extrapolation reduces truncation bias across the board. More importantly, truncation bias is small in both good and bad times. Our extrapolation scheme reduces, if not eliminates, the cyclical component in truncation bias.

To build intuition as to why extrapolation works, we formally describe the experiment. Let $\text{put}(K, \sigma)$ be the Black-Scholes price of a put with strike K and implied volatility σ. Let $IV_p(K)$ be the true implied volatility of a put with strike K. In the left tail, the experiment replaces true put prices with the approximation:

$$\text{put}(K, IV_p(K)) \approx \text{put}(K, IV_p(0.80 \times P)) \text{ for } K \leq 0.80 \times P.$$

The notation and approximation are analogous for calls. In the right tail, the experiment replaces true call prices with the approximation:

$$\text{call}(K, IV_c(K)) \approx \text{call}(K, IV_c(1.20 \times P)) \text{ for } K \geq 1.20 \times P.$$

The success of this approximation depends on two factors. This first is the wedge between near-the-money and deep out-of-the-money volatility. The second is the sensitivity of Black-Scholes prices to volatility. This sensitivity approaches zero in both integration limits:

$$\lim_{K \to 0} \frac{\partial \, \text{put}(K, \sigma)}{\partial \sigma} = 0 \qquad \lim_{K \to \infty} \frac{\partial \, \text{call}(K, \sigma)}{\partial \sigma} = 0.$$

This implies that what matters is not *how* we extrapolate but rather *whether* we extrapolate; that is, the wedge is second-order.

[6] We compute SVJ prices in Matlab via the `optByBatesNI` function.

The analysis above suggests that truncation bias leads to underestimates of forward rates, especially in bad times, but that extrapolation can reduce this bias, especially its cyclical component. The analysis is somewhat silent on forecast errors because we did not take strong stand on the dynamics on the underlying state variable. To make progress on this front, we must turn to the data, which we do so below.

Data. We next analyze truncation bias in the data. To motivate the analysis, we note that there is business-cycle variation in the integral's support. In bad times, stock prices decrease, and this shifts the distribution of strikes upward. Figure A2 visualizes this point in the U.S. sample. This suggests that truncation bias might be able to generate systematic measurement error, which is required for measurement error to explain forecast-error predictability.[7]

To better understand the relevance of this threat, Table A3 examines alternative integration bounds. To build intuition, the top subpanel artificially truncates the volatility surface. The first row truncates the volatility surface at the 25% out-of-the-money strike. Let K_{min} be the minimum put strike in the data. The lower integration bound is

$$\underline{K} = \max\left\{K_{min}, 0.75 \times P_t\right\}.$$

The notation and bound are analogous for calls. Let K_{max} be the maximum call strike in the data. The upper integration bound is

$$\overline{K} = \min\left\{K_{max}, 1.25 \times P_t\right\}.$$

In other words, at best, the first row evaluates the integral in (7) from $\underline{K} = 0.75 \times P_t$ and $\overline{K} = 1.25 \times P_t$, but the bounds might be even shallower, depending on the availability of option prices. The next four rows consider deeper but otherwise analogous bounds. The sixth row evaluates the integral over all observable strikes. Each of these bounds naturally varies both by time and maturity with the availability of option prices.

When considering very narrow truncation limits, our results for risk premia are statistically less strong, which is somewhat expected given that this induces severe truncation bias in the approximated integral. More generally, with shallow bounds, forecast errors are relatively large on average but less predictable. With deep bounds, forecast errors are relatively small on average but more predictable. The fact that our results become weaker following the artificial truncation suggests that the limited availability of strikes does not mechanically produce our results – in fact, such limitations in the data would weaken rather than strengthen our results.

As mentioned above, for measurement error (which includes, but is not limited to, truncation bias) to explain the results, we would have to *overestimate* forward rates in bad times. This upward bias would mechanically generate predictably negative forecast errors. But the experiment above suggests that in the presence of measurement error driven bias truncation bias, we would likely *underestimate* forward rates in bad times. Figure A3 visualizes this point by showing how the estimated forward and spot risk premia change under the different integration bounds. Measurement error therefore does not seem to help explain the results, either quantitatively as in the table or even qualitatively, as it works in the wrong direction.

The bottom subpanel extrapolates the volatility surface. The first row considers static integration

[7] In contrast, neither discretization nor interpolation bias varies with the business cycle. The spacing of option strikes is typically time-invariant. The availability of option maturities typically varies deterministically.

bounds, following a similar robustness check in Gormsen and Jensen (2025):

$$\left[\underline{K}^{(n)}, \overline{K}^{(n)}\right] = \begin{cases} [0.75, 1, 25] \times P_t & n \in \{1, 2\} \\ [0.55, 1.45] \times P_t & n \in \{3, 4, 5\} \\ [0.35, 1.65] \times P_t & n \in \{6, 9\} \\ [0.20, 1.80] \times P_t & n \in \{12\}. \end{cases}$$

These bounds vary by maturity. This variation is logical because deep out-of-the-money options have more time value at longer maturities. The second row considers dynamic integration bounds, again following a similar robustness check in Gormsen and Jensen:

$$\underline{K}^{(n)} = \max\left\{0.10, 1.00 - 5\sigma_t^{(n)}\sqrt{\tau}\right\} \times P_t \qquad \overline{K}^{(n)} = \min\left\{2.00, 1.00 + 5\sigma_t^{(n)}\sqrt{\tau}\right\} \times P_t,$$

where $\sigma_t^{(n)}$, the price of the volatility contract in Bakshi, Kapadia, and Madan (2003), proxies for market volatility:

$$\begin{aligned} \left(\sigma_t^{(n)}\sqrt{\tau}\right)^2 &= \frac{1}{R_f}\,\mathbb{E}_t^*\left[(\ln R)^2\right] \\ &= \int_0^{P_t} \frac{2\left(1 + \ln\left[\frac{P_t}{K}\right]\right)}{K^2}\,\text{put}(K)dK + \int_{P_t}^{\infty} \frac{2\left(1 + \ln\left[\frac{P_t}{K}\right]\right)}{K^2}\,\text{call}(K)dK. \end{aligned} \tag{A11}$$

These bounds vary by time with volatility. This variation is logical because deep out-of-the-money options are more expensive in bad times. The third row considers the baseline integration bounds, as discussed in Appendix B.2. Regression slopes and average errors are quantitatively consistent across all extrapolation schemes, consistent with the idea above that what matters is not how we extrapolate but rather whether we extrapolate. This further helps alleviate concerns about the specific integration bounds used in our baseline: observations very deep in the tails contribute little mass to the LVIX integral,[8] consistent with the theory discussed just above.

C.2 Alternative Measures

The appendix considers robustness checks where we use alternative choices to measure spot rates, forward rates, and forecast errors. Some of these choices are motivated by liquidity. As an example, if liquidity were an issue, then we would expect use of bid/ask prices to significantly alter the results (this is not the case). Other choices are motivated as checks on how exactly we fit a volatility surface to the data. As an example, the SVI surface below explicitly imposes no-arbitrage on the surface (which does not seem to matter either).

Table A4 presents the results. Regression slopes and average errors are quantitatively robust to these choices in all cases, while maintaining their statistical significance in most cases.

Liquidity Filters. The top subpanel repeats the analysis with additional liquidity filters. The second row considers an outlier filter, following similar filters in Constantinides, Jackwerth, and Savov (2013) and Beason and Schreindorfer (2022). On each date and separately for puts/calls, we first fit a quadratic function to implied volatilities in terms of moneyness K/P and time-to-maturity.

[8] To see this directly (without the need to extrapolate), one can consider the Euro Stoxx 50, which has a relatively dense grid of deep out-of-the-money options. At the 6-month horizon, the region $1.65 \leq K/P_t \leq 2.00$ contributes at most five basis points to the integral (with an average contribution near zero).

To minimize the effect of deep out-of-the-money, short/long-maturity options, we only use options with moneyness $0.65 \leq {}^{K}/_{P} \leq 1.35$ and maturity $14 \leq \tau \leq 365$ days. We then drop influential observations via Cook's Distance. The third row considers an open interest filter. We drop options with zero open interest, as seen in Panel B of Figure A11. We do not have open interest data before 1996. The fourth row combines the outlier and open interest filters.

Bid/Ask Prices. The bottom subpanel repeats the analysis with bid/ask prices, following similar robustness checks in Martin (2017) and Gao and Martin (2021). We only have bid/ask prices in the U.S. sample. The first row reports the baseline results with the bid-ask midpoint. The second row repeats the analysis with bid prices, the third ask prices.

Volatility Surface. The second-to-last row in the top subpanel repeats the analysis with the interpolated volatility surface from OptionMetrics. OptionMetrics provides interpolated Black-Scholes implied volatilities on a constant moneyness/maturity grid.[9]

SVI Surface. The last row in the top subpanel repeats the analysis with the stochastic volatility inspired (SVI) surface from Jim Gatheral at Merrill Lynch.[10] Our implementation of the SVI surface closely follows Berger, Dew-Becker, and Giglio (2020) and Beason and Schreindorfer (2022). We parameterize squared Black-Scholes implied volatilities with the function

$$\sigma_{BS}^2(t,\kappa,\tau) = a + b\left(\rho(\kappa - m) + \sqrt{(\kappa - m)^2 + \sigma^2}\right), \tag{A12}$$

where κ is standardized forward moneyness

$$\kappa = \frac{\ln K - \ln F_t^{(n)}}{\sigma_t^{(n)}\sqrt{\tau}},$$

$\sigma_t^{(n)}$ proxies for the risk-neutral volatility of the market return as in (A11), and each parameter is a linear function of time-to-maturity (e.g., $a = a_0 + a_1\tau$).

On each date, we estimate parameters $\theta = (a_0, a_1, b_0, b_1, \rho_0, \rho_1, m_0, m_1, \sigma_0, \sigma_1)$ that minimize the implied volatility RMSE between the surface (A12) and the data, subject to standard no-arbitrage constraints: option prices are nonnegative and monotonic/convex in K. We check these constraints on a grid with moneyness between $-20 \leq \kappa \leq 0.50$ for puts, between $-0.50 \leq \kappa \leq 10$ for calls, and maturities $\tau = 30, 60, 91, 122, 152, 182, 273, 365$ days. We estimate the surface with outlier-filtered, as discussed above, out-of-the-money puts/calls: puts with $\kappa \leq 0$ and calls with $\kappa \geq 0$. We estimate the surface separately for puts/calls and separately for short/long-maturity options: $14 \leq \tau \leq 122$ days and $122 < \tau \leq 365$ days, respectively.[11]

C.3 Additional Robustness Checks

This appendix examines additional empirical exercises related to measurement error. We exploit cross-sectional variation in liquidity across countries and across horizons as well as time-series

[9] The literature often uses this surface for American-exercise options because OptionMetrics reports an equivalent, European-exercise, implied volatility (see, for example, Kelly, Lustig, and Van Nieuwerburgh 2016 and Martin and Wagner 2019).

[10] For more details, see Gatheral and Jacquier (2011, 2014). For a textbook treatment, see Gatheral (2011).

[11] For more details about no-arbitrage violations, see Aït-Sahalia and Duarte (2003).

variation in liquidity in the U.S. sample. We discuss each in turn.

This empirical evidence shows that liquidity-driven measurement error, in fact, weakens our results. This is because illiquidity biases our estimates of forward rates downwards, not upwards as required for measurement error to generate spurious results. This evidence makes us confident that our results on forward rates and forecast errors are driven by the true underlying process of these variables and are very unlikely to be an artifact of measurement error.

Split-Sample Regressions. The first piece of evidence comes from using time variation in the liquidity of option markets in the U.S. sample. Option markets have generally become more liquid over time — on any given trading day, there are literally thousands more options in 2021 than in 1990. More concretely, the surface is more dense, as seen in Figure A14, and the surface extends further into the tails, as seen in Figure A2.

Table A5 reports the results. In the first half, when measurement error is more severe, forecast errors are less predictable. In the second half, when measurement error is less severe, forecast errors are more predictable, even without NBER recessions. That is, our results are stronger in the latter part of our sample. While things other than liquidity have also changed over time, this result similarly suggests that measurement error biases us against our result, and that observing a complete and more liquid set of option prices would strengthen our results.

Alternative Horizons. The next piece of evidence comes from using cross-sectional variation in liquidity across horizons. Short-maturity options (less than 3 months) are substantially more liquid than long-maturity options (more than 3 months), not only in the U.S. sample but also worldwide.

Table A6 considers short horizons: $2 \leq n + m \leq 3$. At these horizons, measurement error is less of a concern. The surface is more dense and extends further into the tails, as seen in Figure A14 and A2. Moreover, the assumptions that the expectations hypothesis holds (see Section 2.2 for more details) and that dividends are known ex ante (see Section 3.1.2 for more details) are more reasonable at short horizons. Our results continue to hold at shorter horizons. This finding reinforces the idea that measurement error can only weaken our results.

Table A7 considers longer horizons: $4 \leq n + m \leq 12$ (the baseline horizon is $n = m = 6$ in the bottom subpanel). At these horizons, measurement error remains a concern. That said, the results continue to hold at these horizons. Holding $n + m$ fixed, forecast errors are relatively small on average and less predictable with small n, relatively large on average and more predictable with large n.

Alternative Samples. The last piece of evidence arises from leveraging cross-country differences in liquidity in the options market. Some countries in our sample have relatively illiquid options markets (like Australia or Spain), while others have very liquid markets (like Germany, the Euro Stoxx 50, and of course, the U.S.). This is especially true when considering the main sample of 10 exchanges versus the full sample of 20 exchanges, as shown in Table A1, which were explicitly categorized on the basis of liquidity. We show that our results are stronger in the most liquid option markets. This finding suggests that if measurement error influences our results, it does so by *weakening* our results and biases us towards finding no effects.

As motivation, Figure A15 visualizes the relationship between spot and forward rates in the global sample, analogous to Figure 2 in the U.S. sample. Table A8 reports the corresponding results. Given liquidity concerns, we make two important changes here relative to the baseline analysis. First, we focus on horizons substantively shorter than the baseline analysis because, as discussed above, there is even less liquidity at long horizons in the non-U.S. sample and especially in the

less-developed option markets considered in this table. So, while liquidity remains a concern in the less-developed markets, it is probably less slightly severe at shorter horizons. Second, we integrate over only observable option prices (that is, we do not extrapolate the surface into the tails as in the baseline analysis). We did not want to spuriously extrapolate the surface and the analysis above in which we consider alternative integration bounds suggests that this is likely to be a conservative approach (that is, bias the results towards the rational expectations null). The table reports results that are quantitatively similar to, but at times somewhat weaker than, that in the main sample. That said, the fact that the results are not stronger in the full sample pushes against the notion that illiquidity in itself can produce rejections of rationality.

As an additional test, we also find that the slopes are substantively weaker — that is, closer to rational expectations null — in exchanges with more illiquid markets, further suggesting that liquidity-driven measurement error cannot spuriously produce significant results. Unlike the full sample analysis above, we conduct this analysis within the main sample and for the baseline horizon, so this likely speaks better to results as a whole. We briefly outline this additional but unreported robustness check. Our proxy for option liquidity is the share of long-maturity options with positive open interest. The cross-exchange ordering of liquidity is reasonable. The usual suspects, like the SPX, SX5E, and DAX, are the most liquid. With this proxy, we examine the cross-exchange relationship between liquidity and the Mincer-Zarnowitz and error-predictability regression slopes. For both slopes, we find a strong negative correlation. Our takeaway, once again, is that that illiquidity works against the results: exchanges with less liquidity have slopes closer to the rational expectations null.

D Additional Empirical Results

D.1 Power Utility Regressions

This appendix derives the power utility analogue to the LVIX in Section 4.1.5. To do so, we apply results from Breeden and Litzenberger (1978) and Martin (2017). We omit time and time-to-maturity dependence throughout for simplicity.

Lemma A1 (Spanning). *For any α and β,*

$$\frac{1}{R_f}\,\mathbb{E}_t^*\left[R^\alpha\,(\ln R)^\beta\right] = R_f^{\alpha-1}\,(\ln R_f)^\beta + \int_0^F \omega(\alpha,\beta)\,\text{put}(K)dK + \int_F^\infty \omega(\alpha,\beta)\,\text{call}(K)dK,$$

where

$$\omega(\alpha,\beta) = -\frac{\alpha\,(1-\alpha)\,m^\beta + \beta\,(1-2\alpha)\,m^{\beta-1} + \beta\,(1-\beta)\,m^{\beta-2}}{P_t^2}\left(\frac{K}{P_t}\right)^{\alpha-2} \tag{A13}$$

and $m = \ln K - \ln P_t$.

As is well-known, under standard regularity conditions, we can compute the price of any function of the index price via a replicating portfolio of bonds, stocks, and options. We simply apply this result to the function $R^\alpha\,(\ln R)^\beta$, which is useful for power utility expectations below.[12]

[12]Lemma A1 clarifies the links among several volatility indexes. The VIX index from the CBOE is a function of $\mathbb{E}_t^*[\ln R]$, the SVIX index from Martin (2017) a function of $\mathbb{E}_t^*\left[R^2\right]$, and the LVIX index from Gao and Martin (2021) a function of $\mathbb{E}_t^*[R\ln R]$.

Proposition A1 (Power Utility). *From the standpoint of an unconstrained power utility investor fully invested in the market,*

$$\mathbb{E}_t[\ln R] - \ln R_f = \frac{\mathbb{E}_t^*[R^\gamma \ln R]}{\mathbb{E}_t^*[R^\gamma]} - \ln R_f, \tag{A14}$$

where

$$\frac{1}{R_f}\,\mathbb{E}_t^*[R^\gamma \ln R] = R_f^{\gamma-1} \ln R_f + \int_0^F \omega(\gamma, 1)\,\text{put}(K)dK + \int_F^\infty \omega(\gamma, 1)\,\text{call}(K)dK, \tag{A15}$$

and

$$\frac{1}{R_f}\,\mathbb{E}_t^*[R^\gamma] = R_f^{\gamma-1} + \int_0^F \omega(\gamma, 0)\,\text{put}(K)dK + \int_F^\infty \omega(\gamma, 0)\,\text{call}(K)dK, \tag{A16}$$

and γ is the investor's risk aversion.

The LVIX is a special case of (A14) with $\gamma = 1$, and so the mechanics under power utility are similar, if only messier, to that under log utility. However, there is one caveat: as risk aversion γ increases, the weights on deep out-of-the-money call options in (A13) become untenably large. Since these options are largely unobservable, we can only realistically measure expectations for a $\gamma \leq 3$ investor in practice.

Armed with equity premia from the standpoint of a power utility investor, we can compute spot rates, forward rates, and forecast errors in the usual way. Table A9 reports regression slopes and average errors for different values of risk aversion. Figure A16 visualizes the results. See Section 4.1.5 for a more thorough discussion.

D.2 Long-Horizon Forecast Errors

This appendix provides details on the forecast-error quantification in Section 5.1.

For the quantification, we re-estimate spot rates, forward rates, and forecast errors at longer horizons (up to $m + n = 8$ years) for the Euro Stoxx 50 (SX5E). The sample runs from September 2005 through September 2014 (beyond which we cannot yet observe realized forecast errors). The combinations of m and n (in months) can be seen in Table A10.

We are only able to do this analysis for Euro Stoxx 50. No other exchange has comparably long-maturity options available for such a long period. The only other exchange with such long maturities is the FTSE 100, but this sample only starts in 2014. More importantly, long-maturity options are liquid for the SX5E: the share of contracts with positive open interest is very consistent for medium (1 to 3 years) and long (3 to 10 years) maturities. In contrast, for the FTSE 100, there is a severe decline in the relative liquidity of long-maturity options (that is, almost no liquidity as per open interest). A few exchanges in the main sample do have option with maturities up to 5 years, but again, the liquidity of these options is suspect, rendering them unusable, at least for this analysis.

For each such combination of m and n, we predict forecast errors as in (9) using a regression of realized forecast errors on shorter-horizon forward rates; we use the $n - 12 \times 12$ forward rate (with horizons again now in months) for $n \geq 24$, and for $n = 12$ we use the 6×6 rate. After obtaining these predicted forecast errors, we calculate a decay parameter for each date's forecast errors, $\phi_t^{(n,m)}$, as the ratio of estimated $\mathbb{E}_t[\tilde{\varepsilon}_{t+n}^{(m)}]$ to $\mathbb{E}_t[\tilde{\varepsilon}_{t+12}^{(12)}]$ for each available $m, n > 12$. This decay specification builds on the one used by De la O and Myers (2021, eq. (13)) for expected returns, but we estimate it directly for each date t (whereas they use a full-sample regression for one horizon).

The entries of Table A10 report the median decay parameter over all t for each combination of m and n. In all cases the estimates are close to or above 1. Assuming that predictable forecast errors are permanent at all horizons might be thought of as providing an estimate of their maximal possible effect. That said, when we estimate the decay parameter in the U.S. (at shorter horizons, unreported), we in fact generally obtain estimates greater than 1, suggesting that setting $\phi^{(n,m)} = 1$ may, if anything, be slightly conservative in the U.S. sample.

E Model Details

E.1 Calibration Implementation

Fundamentals. We measure fundamentals with option-implied volatility (variance, not standard deviation). We omit time and horizon dependence below for simplicity. From the standpoint of an unconstrained log utility investor fully invested in the market, the conditional variance of the 3-month market return is:

$$x_t \equiv \sigma_t^2\big(\ln R\big) = \mathbb{E}_t\big[(\ln R)^2\big] - \big(\mathbb{E}_t\big[\ln R\big]\big)^2 = \frac{\mathbb{E}_t^*\big[R\,(\ln R)^2\big]}{\mathbb{E}_t^*\big[R\big]} - \left(\frac{\mathbb{E}_t^*\big[R \ln R\big]}{\mathbb{E}_t^*\big[R\big]}\right)^2.$$

As before, we consider a log utility investor (Martin 2017) and compute risk-neutral expectations via Lemma A1. The objective volatility dynamics in (16) are

ϕ_1	ϕ_2	ϕ_3	$\overline{x}$	σ_e
0.96	−0.27	0.17	0.98	0.36
(0.05)	(0.07)	(0.05)	(0.14)	(0.01)

The units are non-annualized percentage points. Standard errors are from the simulations below.[13]

Simulations. We evaluate the model via Monte Carlo simulations. The steps are as follows:

1. We simulate the dynamics of volatility via (16). We simulate 100,000 artificial samples of length $T = 378$ months. In each artificial sample, we use a burn-in period of 100 years.

2. We compute forecasts of future volatility via (17), but we replace the objective long-term mean $\overline{x}$ with the misperceived counterpart in (21). In each artificial sample, we initialize the misperceived mean at $\overline{x}$. When $\theta_F > 0$, these forecasts are distorted by forward rate bias; $\theta_F = 0$ nests rationality.

3. We map forecasts of future volatility to forecasts of future short rates via (19), but we replace the objective expectation $\mathbb{E}[\cdot]$ with the subjective counterpart $\mathbb{E}^\theta[\cdot]$ from the previous step. We estimate the mapping in (19) from a regression of contemporaneous short rates on volatility, as in (18).

4. We compute perceptions of current short rates via (22). When $\theta_S \neq 0$, these perceptions are distorted by short rate bias; $\theta_S = 0$ nests rationality.

5. We compute current long-term spot rates via (20), but we again replace the objective expectation $\mathbb{E}[\cdot]$ with the subjective counterpart $\mathbb{E}^\theta[\cdot]$ from the previous two steps.

[13] We note that any measure of volatility would produce qualitatively similar results: what matters is not the particular measure but rather the mapping to risk premia.

With the term structure of spot rates in hand, we can compute forward rates and forecast errors in the usual way.

E.2 Discussion: A Trilemma for Expectation Errors

This appendix continues the discussion in Section 6.3 on how different moments of the data are tied together by the cyclicality of forecast errors.[14] We begin with the Campbell-Shiller price-dividend decomposition in (11). Assume that the expectations $\mathbb{E}_t[\cdot]$ in that decomposition refer to agents' subjective beliefs, and $p_t - d_t$ is the observed log price-dividend ratio. Now consider an alternative economy in which all agents have rational expectations. For arbitrary equilibrium variable x_t in the observed data, denote the corresponding variable in the alternative RE economy by x_t^{RE}. Define the wedge between these two variables to be $\widetilde{x}_t = x_t - x_t^{RE}$. For example, $\widetilde{p_t - d_t}$ is the wedge between the observed price-dividend ratio and the one that would be observed in the alternative economy with RE. Up to a constant, it satisfies

$$\widetilde{p_t - d_t} = \widetilde{CF}_t - \widetilde{\mathcal{F}}_t - \widetilde{RF}_t. \tag{A17}$$

Assume for simplicity that $\widetilde{RF}_t = 0$. The following variance decomposition for the price-dividend wedge therefore holds:

$$\operatorname{var}\left(\widetilde{p_t - d_t}\right) = \operatorname{var}\left(\widetilde{CF}_t\right) + \operatorname{var}\left(\widetilde{\mathcal{F}}_t\right) - 2\operatorname{cov}\left(\widetilde{CF}_t, \widetilde{\mathcal{F}}_t\right). \tag{A18}$$

Alternatively, one can also use the following decomposition given (A17):

$$\operatorname{var}\left(\widetilde{p_t - d_t}\right) = \operatorname{cov}\left(\widetilde{p_t - d_t}, \widetilde{CF}_t\right) - \operatorname{cov}\left(\widetilde{p_t - d_t}, \widetilde{\mathcal{F}}_t\right). \tag{A19}$$

The wedges $\widetilde{CF}_t$ and $\widetilde{\mathcal{F}}_t$ can be understood as expectation errors along the lines considered in Section 6: if subjective expectations are too high relative to RE, then the wedge will be positive (and forecast errors, defined as realized − forecast, are likely to be negative). According to either of the decompositions in (A18)–(A19), therefore, one must choose from at most two of the following three features of any model of expectation errors:

1. Volatile expectation errors for returns (and/or fundamentals)
2. Volatile price-dividend ratio relative to a rational benchmark
3. Countercyclical return expectation errors (positive return expectation errors in bad times)

For example, if excessively positive cash-flow and return forecast revisions occur in good times (after positive news), then $\operatorname{cov}\left(\widetilde{CF}_t, \widetilde{\mathcal{F}}_t\right) > 0$ in (A18). Alternatively, in the version expressed in (A19), positive comovement between price-dividend and forward-rate wedges similarly detracts from a model's ability to generate volatile $\widetilde{p_t - d_t}$. This form of overreaction to *realized outcomes* (cash flows and/or returns) may be intuitively appealing, but it limits a model's ability to speak to variation in the price-dividend ratio through expectation errors alone.[15]

[14] This discussion builds on Campbell (2017), who introduces related trilemmas for present value and portfolio choice.

[15] For example, Nagel and Xu (2022) obtain a price-dividend ratio volatility about 50% lower than that observed in the data (see their Table 5). Similarly, De la O and Myers (2021) report that in the model of Barberis et al. (2015), "movements in dividend change expectations are almost completely negated by movements in price change expectations. This leads to low variation in the price-dividend difference" (p. 1370);

Our empirical results, and our model of expectation errors, instead suggest overreaction of forward rates to fundamentals, rather than realized returns. Unlike realized returns, we find that spot and forward rates *increase* in bad times. The negative covariance between fundamental news and return expectation errors in principle allows for a volatile price-dividend ratio.

Campbell (2017) provides a related discussion of the Barberis et al. (2015) results.

Appendix Tables and Figures

Table A1
Option Sample

This table reports the country or index name, the abbreviation, the underlying index, the sample period, and the sample length in months for each exchange. The last column indicates whether the exchange is in the main sample. See Appendix B.1 for more details.

Name	Abbrv	Index	Start	End	Length	Main
North America						
United States	USA	S&P 500	199001	202112	384	Y
Europe						
Belgium	BEL	BEL 20	200201	202109	228	
Switzerland	CHE	SMI	200201	202109	237	Y
Germany	DEU	DAX	200201	202109	237	Y
Spain	ESP	IBEX 35	200610	202109	180	Y
Finland	FIN	OMXH25	200201	202109	237	
France	FRA	CAC 40	200304	202109	222	Y
United Kingdom	GBR	FTSE 100	200201	202109	237	Y
Italy	ITA	FTSE MIB	200610	202109	180	Y
Netherlands	NLD	AEX	200201	202109	219	
Sweden	SWE	OMXS30	200705	202109	173	
Pan-Europe						
Euro Stoxx 50	SX5E	SX5E	200201	202109	237	Y
Stoxx Europe 50	SX5P	SX5P	200201	202109	237	
Stoxx Europe 600	SXXP	SXXP	200509	202109	193	
Asia-Pacific						
Australia	AUS	ASX 200	200401	202104	208	Y
China	CHN	HSCEI	200601	202104	184	
Hong Kong	HKG	Hang Seng	200601	202104	184	Y
Japan	JPN	Nikkei 225	200405	202104	204	
Korea	KOR	KOSPI 200	200407	202104	202	
Taiwan	TWN	TAIEX	200510	202104	187	

Table A2
Summary Statistics

This table reports summary statistics for option-based (Panel A) and survey-based (Panel B) expectations. The expectations are forward rates and the corresponding realized spot rates for risk premia (on the left) and expected returns (on the right). The option-based horizon is the 6×6-month forecast error, the Livingston horizon is the 6×6-month forecast error, and the CFO horizon is the 1×9-year forecast error. The units are annualized percentage points. The option-based sample is is the longest available for each exchange. The Livingston sample is half-yearly from 06/1992 to 06/2021 for forward rates and from 12/1992 to 12/2021 for realized spot rates. The CFO sample is quarterly from 12/2001 to 12/2018 for forward rates and from 12/2002 to 12/2019 for realized spot rates. See Section 4 for more details.

	Panel A. Option-Based Expectations								
	Forward RP		Spot RP		Forward ER		Spot ER		
	Mean	StDev	Mean	StDev	Mean	StDev	Mean	StDev	Length
North America									
USA	2.15	0.99	2.17	1.40	5.44	2.32	5.04	2.41	378
Europe									
BEL	2.56	2.22	2.42	2.07	4.13	2.79	3.59	2.82	213
CHE	1.88	0.80	1.96	1.34	2.60	1.50	2.26	1.85	231
DEU	2.63	1.07	2.85	1.86	4.27	2.12	4.10	2.74	231
ESP	2.89	1.17	3.37	1.83	4.19	2.19	4.19	2.73	168
FIN	2.38	1.85	2.79	2.21	4.02	2.65	4.03	2.85	231
FRA	2.44	1.04	2.57	1.56	3.97	2.07	3.71	2.42	215
GBR	2.12	1.00	2.21	1.51	4.76	2.13	4.33	2.59	224
ITA	3.17	1.35	3.60	1.67	4.42	2.23	4.39	2.40	174
NLD	2.43	1.26	2.85	2.18	3.95	2.40	3.93	3.20	202
SWE	2.44	1.41	2.79	1.80	3.77	2.68	3.79	2.83	160
Pan-Europe									
SX5E	2.65	1.08	2.89	1.83	4.29	2.10	4.14	2.69	231
SX5P	2.11	1.48	2.23	1.62	3.75	2.51	3.47	2.64	231
SXXP	2.05	1.53	2.14	1.63	3.44	2.57	3.12	2.65	185
Asia-Pacific									
AUS	1.84	1.20	1.97	1.39	5.95	2.39	5.65	2.65	197
CHN	3.90	3.29	4.24	4.01	5.92	3.64	5.61	4.42	178
HKG	2.85	1.93	2.98	2.56	4.86	2.26	4.35	2.98	178
JPN	2.60	1.57	2.93	2.20	3.15	1.76	3.21	2.35	197
KOR	2.14	1.85	2.23	2.16	5.40	2.95	5.13	3.02	194
TWN	2.36	1.45	2.39	1.90	3.84	1.70	3.37	2.11	181
	Panel B. Survey-Based Expectations								
	Forward RP		Spot RP		Forward ER		Spot ER		
	Mean	StDev	Mean	StDev	Mean	StDev	Mean	StDev	Length
Livingston Survey									
Option	2.16	1.01	2.08	1.20	5.20	2.16	4.79	2.24	59
Survey	3.15	4.96	3.52	5.35	5.73	3.81	5.84	4.14	59
CFO Survey									
Option	2.28	1.08	2.21	1.51	4.21	1.45	3.95	1.92	68
Survey	3.37	0.57	3.46	0.57	6.77	0.77	6.52	0.68	68

Table A3
Alternative Integration Bounds

This table reports estimates with alternative integration bounds for option-based risk premia (Panel A) and expected returns (Panel B). Mincer-Zarnowitz regressions test $H_0\colon \beta_1 = 1$, as in Table 2. The average forecast error tests $H_0\colon \bar{\varepsilon}_t = 0$, as in Table 4. Error-predictability regressions test $H_0\colon \beta_1 = 0$, as in Table 5. The horizon is the 6-month spot rate, 6 months from now. The units are annualized percentage points. All regressions include exchange fixed effects and compute a within R^2. Standard errors are clustered by exchange and date. The sample is the longest available for each exchange in the main sample. See Appendix C.1 for more details.

	Panel A. Risk Premia $\tilde{\mu}^{(6)}_{t+6}$											
	Mincer-Zarnowitz				Average Error			Error Predictability				
	β_1	$se(\beta_1)$	p-val	R^2	$\tilde{\varepsilon}_t$	$se(\tilde{\varepsilon}_t)$	p-val	β_1	$se(\beta_1)$	p-val	R^2	N
Without Extrapolation												
Truncation: $0.75 \leq {}^{K}/_{P} \leq 1.25$	0.92	0.12		0.19	0.44	0.088	***	0.066	0.040		0.01	2140
Truncation: $0.65 \leq {}^{K}/_{P} \leq 1.35$	0.78	0.091	**	0.18	0.34	0.094	***	-0.019	0.039		0.00	2139
Truncation: $0.55 \leq {}^{K}/_{P} \leq 1.45$	0.68	0.074	***	0.17	0.26	0.097	**	-0.082	0.041	*	0.01	2137
Truncation: $0.45 \leq {}^{K}/_{P} \leq 1.55$	0.63	0.065	***	0.16	0.22	0.099	*	-0.12	0.042	**	0.02	2140
Truncation: $0.35 \leq {}^{K}/_{P} \leq 1.65$	0.59	0.059	***	0.15	0.20	0.10	*	-0.15	0.044	***	0.03	2138
Observable Strike Prices	0.56	0.053	***	0.15	0.19	0.10	*	-0.17	0.043	***	0.04	2140
With Extrapolation												
Static Integration Bounds	0.56	0.056	***	0.15	0.14	0.10		-0.15	0.041	***	0.04	2244
Dynamic Integration Bounds	0.56	0.055	***	0.15	0.16	0.11		-0.17	0.046	***	0.03	2241
Baseline: $0.10 \leq {}^{K}/_{P} \leq 2.00$	0.56	0.055	***	0.15	0.17	0.11		-0.16	0.047	***	0.03	2227
	Panel B. Expected Returns $\mu^{(6)}_{t+6}$											
	Mincer-Zarnowitz				Average Error			Error Predictability				
	β_1	$se(\beta_1)$	p-val	R^2	ε_t	$se(\varepsilon_t)$	p-val	β_1	$se(\beta_1)$	p-val	R^2	N
Without Extrapolation												
Truncation: $0.75 \leq {}^{K}/_{P} \leq 1.25$	1.04	0.052		0.77	-0.0079	0.088		-0.12	0.048	**	0.02	2140
Truncation: $0.65 \leq {}^{K}/_{P} \leq 1.35$	1.02	0.053		0.71	-0.12	0.094		-0.18	0.043	***	0.04	2139
Truncation: $0.55 \leq {}^{K}/_{P} \leq 1.45$	0.99	0.054		0.67	-0.19	0.097	*	-0.23	0.044	***	0.07	2137
Truncation: $0.45 \leq {}^{K}/_{P} \leq 1.55$	0.96	0.055		0.64	-0.23	0.099	**	-0.26	0.045	***	0.09	2140
Truncation: $0.35 \leq {}^{K}/_{P} \leq 1.65$	0.94	0.056		0.63	-0.25	0.10	**	-0.29	0.046	***	0.10	2138
Observable Strike Prices	0.93	0.058		0.61	-0.26	0.10	**	-0.31	0.046	***	0.12	2140
With Extrapolation												
Static Integration Bounds	0.92	0.060		0.60	-0.31	0.100	**	-0.26	0.039	***	0.12	2244
Dynamic Integration Bounds	0.91	0.061		0.59	-0.29	0.10	**	-0.30	0.047	***	0.11	2241
Baseline: $0.10 \leq {}^{K}/_{P} \leq 2.00$	0.91	0.061		0.59	-0.28	0.10	**	-0.29	0.047	***	0.10	2227

Table A4
Alternative Measures

This table reports estimates with alternative measures for option-based risk premia (Panel A) and expected returns (Panel B). Mincer-Zarnowitz regressions test $H_0\colon \beta_1 = 1$, as in Table 2. The average forecast error tests $H_0\colon \bar{\varepsilon}_t = 0$, as in Table 4. Error-predictability regressions test $H_0\colon \beta_1 = 0$, as in Table 5. The horizon is the 6-month spot rate, 6 months from now. The units are annualized percentage points. Panel regressions, in the main sample, include exchange fixed effects, compute a within R^2, and report standard errors clustered by exchange and date. This sample is the longest available for each exchange. Time-series regressions, in the U.S. sample, report Newey-West standard errors with $L = \lceil 1.3 \times T^{1/2} \rceil$ lags and fixed-b p-values, following Lazarus et al. (2018). This sample is from 01/1990 to 06/2021. See Appendix C.2 for more details.

	Panel A. Risk Premia $\tilde{\mu}^{(6)}_{t+6}$											
	Mincer-Zarnowitz				Average Error			Error Predictability				
	β_1	$se(\beta_1)$	p-val	R^2	$\tilde{\varepsilon}_t$	$se(\tilde{\varepsilon}_t)$	p-val	β_1	$se(\beta_1)$	p-val	R^2	N
Main Sample												
Baseline Filters/Surface	0.56	0.055	***	0.15	0.17	0.11		-0.16	0.047	***	0.03	2227
Outlier Filter	0.60	0.055	***	0.17	0.18	0.098		-0.20	0.050	***	0.05	2241
Open Interest Filter: After 199601	0.52	0.057	***	0.14	0.16	0.11		-0.18	0.045	***	0.04	2033
Outlier/Open Interest Filter: After 199601	0.56	0.051	***	0.15	0.19	0.097	*	-0.21	0.050	***	0.06	2040
Volatility Surface: After 199601	0.57	0.051	***	0.17	0.087	0.095		-0.21	0.053	***	0.06	2163
SVI Surface: U.S. and SX5E	0.59	0.047	*	0.17	0.051	0.11		-0.19	0.039		0.04	609
U.S. Sample												
Bid-Ask Midpoint	0.67	0.096	***	0.22	0.021	0.15		-0.17	0.067	**	0.03	378
Bid Prices	0.64	0.099	***	0.21	0.034	0.14		-0.15	0.078	*	0.03	378
Ask Prices	0.66	0.089	***	0.23	0.0051	0.15		-0.18	0.060	***	0.04	378

	Panel B. Expected Returns $\mu^{(6)}_{t+6}$											
	Mincer-Zarnowitz				Average Error			Error Predictability				
	β_1	$se(\beta_1)$	p-val	R^2	ε_t	$se(\varepsilon_t)$	p-val	β_1	$se(\beta_1)$	p-val	R^2	N
Main Sample												
Baseline Filters/Surface	0.91	0.061		0.59	-0.28	0.10	**	-0.29	0.047	***	0.10	2227
Outlier Filter	0.92	0.062		0.62	-0.27	0.098	**	-0.34	0.050	***	0.15	2241
Open Interest Filter: After 199601	0.91	0.062		0.59	-0.26	0.10	**	-0.31	0.043	***	0.12	2033
Outlier/Open Interest Filter: After 199601	0.92	0.064		0.62	-0.24	0.096	**	-0.35	0.048	***	0.16	2040
Volatility Surface: After 199601	0.93	0.065		0.63	-0.34	0.098	***	-0.36	0.052	***	0.16	2163
SVI Surface: U.S. and SX5E	0.89	0.048		0.65	-0.36	0.11		-0.28	0.049		0.10	609
U.S. Sample												
Bid-Ask Midpoint	0.88	0.073		0.71	-0.40	0.17	**	-0.20	0.091	**	0.04	378
Bid Prices	0.87	0.070	*	0.73	-0.38	0.17	**	-0.18	0.11		0.04	378
Ask Prices	0.87	0.076		0.69	-0.41	0.18	**	-0.21	0.077	**	0.05	378

Table A5
Split-Sample Regressions

This table reports estimates in split samples for option-based risk premia (Panel A) and expected returns (Panel B). Mincer-Zarnowitz regressions test $H_0\colon \beta_1 = 1$, as in Table 2. The average forecast error tests $H_0\colon \bar{\varepsilon}_t = 0$, as in Table 4. Error-predictability regressions test $H_0\colon \beta_1 = 0$, as in Table 5. The horizon is the 6-month spot rate, 6 months from now. The units are annualized percentage points. Each regression reports Newey-West standard errors with $L = \lceil 1.3 \times T^{1/2} \rceil$ lags and fixed-b p-values, following Lazarus et al. (2018). See Appendix C.3 for more details.

	Panel A. Risk Premia $\tilde{\mu}^{(6)}_{t+6}$											
	Mincer-Zarnowitz				Average Error			Error Predictability				
	β_1	$se(\beta_1)$	p-val	R^2	$\tilde{\varepsilon}_t$	$se(\tilde{\varepsilon}_t)$	p-val	β_1	$se(\beta_1)$	p-val	R^2	N
U.S. Sample												
Baseline: 199001 to 202106	0.67	0.096	***	0.22	0.021	0.15		-0.17	0.067	**	0.03	378
First Half: 199001 to 200509	0.82	0.12		0.38	0.025	0.15		-0.055	0.074		-0.00	189
Second Half: 200510 to 202106	0.56	0.11	***	0.14	0.017	0.24		-0.22	0.075	**	0.05	189
Second Half: 200907 to 201907	0.50	0.10	***	0.20	-0.40	0.12	***	-0.37	0.089	***	0.16	121
	Panel B. Expected Returns $\mu^{(6)}_{t+6}$											
	Mincer-Zarnowitz				Average Error			Error Predictability				
	β_1	$se(\beta_1)$	p-val	R^2	ε_t	$se(\varepsilon_t)$	p-val	β_1	$se(\beta_1)$	p-val	R^2	N
U.S. Sample												
Baseline: 199001 to 202106	0.88	0.073		0.71	-0.40	0.17	**	-0.20	0.091	**	0.04	378
First Half: 199001 to 200509	0.85	0.081		0.72	-0.58	0.25	**	0.023	0.12		-0.00	189
Second Half: 200510 to 202106	0.92	0.14		0.48	-0.22	0.18		-0.32	0.079	***	0.13	189
Second Half: 200907 to 201907	0.58	0.20	*	0.23	-0.50	0.13	***	-0.47	0.074	***	0.23	121

Table A6
Short-Horizon Regressions

This table reports estimates at short horizons for option-based risk premia (Panel A) and expected returns (Panel B). Mincer-Zarnowitz regressions test $H_0\colon \beta_1 = 1$, as in Table 2. The average forecast error tests $H_0\colon \bar{\varepsilon}_t = 0$, as in Table 4. Error-predictability regressions test $H_0\colon \beta_1 = 0$, as in Table 5. The horizon is the m-month spot rate, n months from now. The units are annualized percentage points. Panel regressions, in the main sample, include exchange fixed effects, compute a within R^2, and report standard errors clustered by exchange and date. This sample is the longest available for each exchange. Time-series regressions, in the U.S. sample, report Newey-West standard errors with $L = \lceil 1.3 \times T^{1/2} \rceil$ lags and fixed-b p-values, following Lazarus et al. (2018). This sample is from 01/1990 to 06/2021. See Appendix C.3 for more details.

		Panel A. Risk Premia $\tilde{\mu}_{t+n}^{(m)}$											
		Mincer-Zarnowitz				Average Error			Error Predictability				
		β_1	$se(\beta_1)$	p-val	R^2	$\tilde{\varepsilon}_t$	$se(\tilde{\varepsilon}_t)$	p-val	β_1	$se(\beta_1)$	p-val	R^2	N
Main Sample													
$n=1$	$m=1$	0.86	0.062	**	0.48	0.068	0.10		-0.17	0.049	***	0.03	2268
$n=1$	$m=2$	0.86	0.055	**	0.53	0.018	0.087		-0.17	0.048	***	0.04	2269
$n=2$	$m=1$	0.71	0.067	***	0.27	0.021	0.13		-0.29	0.067	***	0.06	2269
U.S. Sample													
$n=1$	$m=1$	0.88	0.067		0.52	-0.020	0.066		-0.14	0.075	*	0.02	381
$n=1$	$m=2$	0.89	0.050	**	0.60	-0.071	0.051		-0.12	0.052	**	0.02	382
$n=2$	$m=1$	0.73	0.085	***	0.30	-0.14	0.10		-0.27	0.085	***	0.05	382
		Panel B. Expected Returns $\mu_{t+n}^{(m)}$											
		Mincer-Zarnowitz				Average Error			Error Predictability				
		β_1	$se(\beta_1)$	p-val	R^2	ε_t	$se(\varepsilon_t)$	p-val	β_1	$se(\beta_1)$	p-val	R^2	N
Main Sample													
$n=1$	$m=1$	0.94	0.059		0.67	-0.070	0.11		-0.24	0.051	***	0.05	2268
$n=1$	$m=2$	0.93	0.049		0.73	-0.14	0.086		-0.23	0.048	***	0.07	2269
$n=2$	$m=1$	0.87	0.065	*	0.54	-0.28	0.13	*	-0.40	0.070	***	0.11	2269
U.S. Sample													
$n=1$	$m=1$	0.98	0.024		0.78	-0.15	0.064	**	-0.20	0.058	***	0.04	381
$n=1$	$m=2$	0.97	0.016		0.84	-0.20	0.045	***	-0.15	0.042	***	0.04	382
$n=2$	$m=1$	0.94	0.032	*	0.68	-0.40	0.089	***	-0.32	0.065	***	0.08	382

Table A7
Alternative Horizons

This table reports estimates at alternative horizons for option-based risk premia (Panel A) and expected returns (Panel B). Mincer-Zarnowitz regressions test $H_0\colon \beta_1 = 1$, as in Table 2. The average forecast error tests $H_0\colon \bar{\varepsilon}_t = 0$, as in Table 4. Error-predictability regressions test $H_0\colon \beta_1 = 0$, as in Table 5. The horizon is the m-month spot rate, n months from now. The units are annualized percentage points. All regressions include exchange fixed effects and compute a within R^2. Standard errors are clustered by exchange and date. The sample is the longest available for each exchange in the main sample. See Appendix C.3 for more details.

		Panel A. Risk Premia $\tilde{\mu}_{t+n}^{(m)}$											
		Mincer-Zarnowitz				Average Error			Error Predictability				
		β_1	$se(\beta_1)$	p-val	R^2	$\bar{\varepsilon}_t$	$se(\bar{\varepsilon}_t)$	p-val	β_1	$se(\beta_1)$	p-val	R^2	N
4-Month Horizon: $n+m=4$													
$n=1$	$m=3$	0.90	0.048	*	0.62	0.044	0.073		-0.12	0.040	**	0.03	2269
$n=2$	$m=2$	0.77	0.058	***	0.35	0.055	0.11		-0.20	0.053	***	0.04	2268
$n=3$	$m=1$	0.68	0.065	***	0.20	0.094	0.14		-0.24	0.055	***	0.03	2235
5-Month Horizon: $n+m=5$													
$n=1$	$m=4$	0.94	0.043		0.67	0.067	0.064		-0.075	0.033	*	0.01	2269
$n=2$	$m=3$	0.83	0.053	**	0.42	0.12	0.10		-0.13	0.043	**	0.02	2268
$n=3$	$m=2$	0.74	0.063	***	0.25	0.16	0.13		-0.15	0.049	**	0.02	2241
$n=4$	$m=1$	0.62	0.078	***	0.13	0.27	0.15		-0.19	0.053	***	0.02	2236
6-Month Horizon: $n+m=6$													
$n=1$	$m=5$	0.95	0.037		0.69	0.067	0.058		-0.054	0.029	*	0.01	2269
$n=2$	$m=4$	0.86	0.047	**	0.46	0.14	0.091		-0.094	0.036	**	0.01	2268
$n=3$	$m=3$	0.78	0.058	***	0.30	0.21	0.12		-0.11	0.044	**	0.01	2249
$n=4$	$m=2$	0.67	0.072	***	0.17	0.27	0.14	*	-0.15	0.050	**	0.02	2238
$n=5$	$m=1$	0.57	0.076	***	0.09	0.32	0.17	*	-0.20	0.057	***	0.02	2228
9-Month Horizon: $n+m=9$													
$n=3$	$m=6$	0.81	0.055	***	0.38	0.15	0.087		-0.065	0.036		0.01	2257
$n=4$	$m=5$	0.73	0.066	***	0.26	0.21	0.10	*	-0.10	0.044	**	0.01	2242
$n=5$	$m=4$	0.65	0.071	***	0.17	0.26	0.12	*	-0.14	0.049	**	0.02	2232
$n=6$	$m=3$	0.55	0.071	***	0.10	0.28	0.14	*	-0.17	0.051	***	0.02	2224
12-Month Horizon: $n+m=12$													
$n=3$	$m=9$	0.81	0.049	***	0.44	0.094	0.070		-0.059	0.036		0.01	2258
$n=6$	$m=6$	0.56	0.055	***	0.15	0.17	0.11		-0.16	0.047	***	0.03	2227
$n=9$	$m=3$	0.39	0.097	***	0.05	0.25	0.15		-0.24	0.052	***	0.04	2191

(Continued on the next page)

Table A7
Alternative Horizons (Continued)

		Panel B. Expected Returns $\mu_{t+n}^{(m)}$											
		Mincer-Zarnowitz				Average Error			Error Predictability				
		β_1	$se(\beta_1)$	p-val	R^2	ε_t	$se(\varepsilon_t)$	p-val	β_1	$se(\beta_1)$	p-val	R^2	N
4-Month Horizon: $n+m=4$													
$n=1$	$m=3$	0.96	0.042		0.80	-0.074	0.073		-0.17	0.039	***	0.06	2269
$n=2$	$m=2$	0.90	0.057		0.62	-0.21	0.11	*	-0.30	0.056	***	0.09	2268
$n=3$	$m=1$	0.89	0.068		0.50	-0.26	0.14	*	-0.36	0.059	***	0.08	2235
5-Month Horizon: $n+m=5$													
$n=1$	$m=4$	0.99	0.038		0.84	-0.027	0.063		-0.12	0.033	***	0.04	2269
$n=2$	$m=3$	0.95	0.052		0.69	-0.080	0.097		-0.22	0.046	***	0.06	2268
$n=3$	$m=2$	0.94	0.063		0.57	-0.13	0.12		-0.27	0.053	***	0.06	2241
$n=4$	$m=1$	0.92	0.080		0.45	-0.11	0.14		-0.33	0.057	***	0.06	2236
6-Month Horizon: $n+m=6$													
$n=1$	$m=5$	0.99	0.035		0.86	-0.027	0.057		-0.10	0.029	***	0.03	2269
$n=2$	$m=4$	0.97	0.049		0.73	-0.039	0.086		-0.18	0.040	***	0.05	2268
$n=3$	$m=3$	0.97	0.057		0.63	-0.043	0.11		-0.22	0.048	***	0.05	2249
$n=4$	$m=2$	0.95	0.071		0.52	-0.082	0.13		-0.29	0.052	***	0.06	2238
$n=5$	$m=1$	0.93	0.082		0.42	-0.15	0.15		-0.36	0.059	***	0.07	2228
9-Month Horizon: $n+m=9$													
$n=3$	$m=6$	0.97	0.046		0.73	-0.075	0.082		-0.16	0.036	***	0.05	2257
$n=4$	$m=5$	0.97	0.055		0.66	-0.082	0.096		-0.22	0.040	***	0.06	2242
$n=5$	$m=4$	0.97	0.063		0.59	-0.10	0.11		-0.27	0.046	***	0.07	2232
$n=6$	$m=3$	0.94	0.071		0.51	-0.17	0.13		-0.31	0.053	***	0.08	2224
12-Month Horizon: $n+m=12$													
$n=3$	$m=9$	0.96	0.039		0.78	-0.14	0.067	*	-0.15	0.034	***	0.06	2258
$n=6$	$m=6$	0.91	0.061		0.59	-0.28	0.10	**	-0.29	0.047	***	0.10	2227
$n=9$	$m=3$	0.81	0.077	**	0.41	-0.46	0.15	**	-0.41	0.062	***	0.12	2191

(Continued from the previous page)

Table A8
Alternative Samples

This table reports estimates in alternative samples for option-based risk premia (Panel A) and expected returns (Panel B). Mincer-Zarnowitz regressions test $H_0\colon \beta_1 = 1$, as in Table 2. The average forecast error tests $H_0\colon \bar{\varepsilon}_t = 0$, as in Table 4. Error-predictability regressions test $H_0\colon \beta_1 = 0$, as in Table 5. The horizon is the 1-month spot rate, 2 months from now. The units are annualized percentage points. All regressions include exchange fixed effects and compute a within R^2. Standard errors are clustered by exchange and date. The sample is the longest available for each exchange. See Appendix C.3 for more details.

	Panel A. Risk Premia $\tilde{\mu}^{(6)}_{t+6}$											
	Mincer-Zarnowitz				Average Error			Error Predictability				
	β_1	$se(\beta_1)$	p-val	R^2	$\bar{\tilde{\varepsilon}}_t$	$se(\bar{\tilde{\varepsilon}}_t)$	p-val	β_1	$se(\beta_1)$	p-val	R^2	N
Baseline												
Main: 10 Exchanges	0.76	0.059	***	0.30	0.047	0.13		-0.24	0.059	***	0.04	2198
Full: 20 Exchanges	0.76	0.050	***	0.30	0.14	0.13		-0.24	0.050	***	0.04	4033
Eurozone												
Main: 5 Exchanges	0.73	0.076	**	0.28	0.070	0.14		-0.27	0.076	**	0.05	1040
Full: 8 Exchanges	0.72	0.062	***	0.29	0.12	0.15		-0.28	0.062	***	0.06	1568
Europe												
Main: 7 Exchanges	0.73	0.067	***	0.28	0.057	0.13		-0.27	0.067	***	0.05	1510
Full: 13 Exchanges	0.72	0.054	***	0.29	0.084	0.13		-0.28	0.054	***	0.06	2619
Asia-Pacific												
Main: 2 Exchanges	0.88	0.12		0.36	0.21	0.15		-0.12	0.12		0.01	319
Full: 6 Exchanges	0.86	0.078		0.34	0.36	0.17	*	-0.14	0.078		0.01	1045
Excludes U.S.												
Main: 9 Exchanges	0.76	0.063	***	0.30	0.083	0.13		-0.24	0.063	***	0.04	1829
Full: 19 Exchanges	0.76	0.051	***	0.30	0.16	0.14		-0.24	0.051	***	0.04	3664

	Panel B. Expected Returns $\mu^{(6)}_{t+6}$											
	Mincer-Zarnowitz				Average Error			Error Predictability				
	β_1	$se(\beta_1)$	p-val	R^2	$\bar{\varepsilon}_t$	$se(\bar{\varepsilon}_t)$	p-val	β_1	$se(\beta_1)$	p-val	R^2	N
Baseline												
Main: 10 Exchanges	0.90	0.063		0.57	-0.26	0.12	*	-0.36	0.064	***	0.09	2198
Full: 20 Exchanges	0.89	0.066		0.55	-0.17	0.13		-0.35	0.057	***	0.09	4033
Eurozone												
Main: 5 Exchanges	0.87	0.080		0.53	-0.24	0.14		-0.40	0.085	***	0.11	1040
Full: 8 Exchanges	0.85	0.078		0.53	-0.20	0.15		-0.41	0.071	***	0.12	1568
Europe												
Main: 7 Exchanges	0.87	0.076		0.54	-0.24	0.13		-0.41	0.077	***	0.11	1510
Full: 13 Exchanges	0.86	0.074	*	0.56	-0.23	0.13		-0.42	0.064	***	0.13	2619
Asia-Pacific												
Main: 2 Exchanges	0.96	0.071		0.59	-0.21	0.16		-0.23	0.10		0.03	319
Full: 6 Exchanges	0.95	0.081		0.50	0.036	0.17		-0.21	0.076	**	0.03	1045
Excludes U.S.												
Main: 9 Exchanges	0.89	0.071		0.55	-0.23	0.13		-0.37	0.069	***	0.09	1829
Full: 19 Exchanges	0.88	0.071		0.54	-0.15	0.14		-0.36	0.059	***	0.09	3664

Table A9
Power Utility Regressions

This table reports estimates from the standpoint of an unconstrained power utility investor fully invested in the market for option-based risk premia (Panel A) and expected returns (Panel B). Mincer-Zarnowitz regressions test $H_0\colon \beta_1 = 1$, as in Table 2. The average forecast error tests $H_0\colon \bar{\varepsilon}_t = 0$, as in Table 4. Error-predictability regressions test $H_0\colon \beta_1 = 0$, as in Table 5. The horizon is the 6-month spot rate, 6 months from now. The units are annualized percentage points. Panel regressions, in the main sample, include exchange fixed effects, compute a within R^2, and report standard errors clustered by exchange and date. This sample is the longest available for each exchange. Time-series regressions, in the U.S. sample, report Newey-West standard errors with $L = \lceil 1.3 \times T^{1/2} \rceil$ lags and fixed-b p-values, following Lazarus et al. (2018). This sample is from 01/1990 to 06/2021. See Appendix D.1 for more details.

Panel A. Risk Premia $\tilde{\mu}^{(6)}_{t+6}$

	Mincer-Zarnowitz				Average Error			Error Predictability				
	β_1	$se(\beta_1)$	p-val	R^2	$\bar{\varepsilon}_t$	$se(\bar{\varepsilon}_t)$	p-val	β_1	$se(\beta_1)$	p-val	R^2	N
Main Sample												
$\gamma = 0.75$	0.51	0.059	***	0.13	0.045	0.057		-0.19	0.045	***	0.04	2224
$\gamma = 1.00$	0.56	0.055	***	0.15	0.17	0.11		-0.16	0.046	***	0.03	2220
$\gamma = 1.25$	0.60	0.057	***	0.15	0.36	0.15	**	-0.13	0.050	**	0.02	2215
$\gamma = 1.50$	0.62	0.062	***	0.16	0.59	0.20	**	-0.10	0.054	*	0.01	2206
$\gamma = 2.00$	0.64	0.075	***	0.15	1.14	0.29	***	-0.044	0.057		0.00	2181
U.S. Sample												
$\gamma = 0.75$	0.61	0.095	***	0.21	-0.022	0.083		-0.20	0.070	***	0.05	378
$\gamma = 1.00$	0.67	0.096	***	0.22	0.021	0.15		-0.17	0.067	**	0.03	378
$\gamma = 1.25$	0.72	0.099	**	0.23	0.12	0.20		-0.13	0.064	*	0.02	378
$\gamma = 1.50$	0.76	0.10	**	0.24	0.25	0.26		-0.099	0.063		0.01	378
$\gamma = 2.00$	0.85	0.10		0.26	0.57	0.35		-0.048	0.060		0.00	378
$\gamma = 2.50$	0.91	0.10		0.27	0.94	0.44	*	-0.0087	0.057		-0.00	378
$\gamma = 3.00$	0.97	0.10		0.28	1.32	0.52	**	0.022	0.056		-0.00	378

Panel B. Expected Returns $\mu^{(6)}_{t+6}$

	Mincer-Zarnowitz				Average Error			Error Predictability				
	β_1	$se(\beta_1)$	p-val	R^2	ε_t	$se(\varepsilon_t)$	p-val	β_1	$se(\beta_1)$	p-val	R^2	N
Main Sample												
$\gamma = 0.75$	0.93	0.042		0.75	-0.40	0.061	***	-0.42	0.056	***	0.17	2224
$\gamma = 1.00$	0.91	0.061		0.59	-0.28	0.10	**	-0.30	0.046	***	0.11	2220
$\gamma = 1.25$	0.90	0.075		0.49	-0.084	0.15		-0.22	0.048	***	0.07	2215
$\gamma = 1.50$	0.90	0.088		0.43	0.15	0.19		-0.17	0.052	***	0.04	2206
$\gamma = 2.00$	0.88	0.11		0.36	0.69	0.28	**	-0.093	0.057		0.01	2181
U.S. Sample												
$\gamma = 0.75$	0.89	0.061	*	0.84	-0.44	0.14	***	-0.24	0.13	*	0.04	378
$\gamma = 1.00$	0.88	0.073		0.71	-0.40	0.17	**	-0.20	0.091	**	0.04	378
$\gamma = 1.25$	0.87	0.083		0.61	-0.30	0.21		-0.15	0.077	*	0.03	378
$\gamma = 1.50$	0.87	0.090		0.53	-0.17	0.26		-0.12	0.071		0.02	378
$\gamma = 2.00$	0.90	0.096		0.45	0.15	0.34		-0.066	0.063		0.00	378
$\gamma = 2.50$	0.93	0.098		0.41	0.52	0.42		-0.024	0.059		-0.00	378
$\gamma = 3.00$	0.96	0.098		0.39	0.90	0.50	*	0.0077	0.056		-0.00	378

Table A10
Long-Horizon Forecast Errors

This table reports estimates of forecast error decay for option-based risk premia. The time-t decay $\phi_t^{(n,m)}$ is the ratio of long to short-horizon forecast errors:

$$\mathbb{E}_t\left[\tilde{\varepsilon}_{t+n}^{(m)}\right] = \phi_t^{(n,m)}\,\mathbb{E}_t\left[\tilde{\varepsilon}_{t+12}^{(12)}\right].$$

The table below reports the median decay $\phi^{(n,m)}$ by horizon:

$$\phi^{(n,m)} = median\left\{\left|\phi_t^{(n,m)}\right|\right\}.$$

The predicted forecast error $\mathbb{E}_t[\cdot]$ is from a time-series regression of future realized forecast errors on current forward rates: the predictor is the 6×6-month forward rate for $n = 12$ and the $n-12\times 12$-month forward rate for $n \geq 24$. The sample begins in 09/2005 and is the longest available for each horizon in the Eurozone (Euro Stoxx 50). See Appendix D.2 for more details.

	n-months						
m-months	12	24	36	48	60	72	84
12	1.00	1.84	1.52	0.70	1.28	1.74	1.59
24	1.00	1.81	1.55	0.85	1.26	1.94	
36	1.00	1.85	1.63	0.83	1.64		
48	1.00	1.98	1.76	1.35			
60	1.00	1.97	1.93				
72	1.00	2.03					
84	1.00						

Figure A1
Truncation Bias in Theory

This figure reports truncation bias in the Black-Scholes (left panel) and SVJ (right panel) models. Panel A truncates the implied volatility surface at the specified bounds (truncation bounds). Panel B extrapolates the implied volatility surface from the specified bounds (extrapolation bounds). The x-axis units are simple moneyness $^{K}/_{P}$ units from the index price. The y-axis units are non-annualized basis points. The bar units are volatility standard deviations from the forward price: $\frac{K/F-1}{\sigma\sqrt{\tau}}$. Black-Scholes parameters: $P = 100$, $r = 0.05$, $q = 0.00$. SVJ parameters under the risk-neutral measure are from Bakshi, Cao, and Chen (1997):

θ_v	κ_v	σ_v	ρ	μ_J	σ_J	λ
0.040	2.030	0.380	-0.570	-0.050	0.070	0.590

Good times correspond to low volatility ($IV = 0.20$ or $\sqrt{v} = 0.20$), bad times to high volatility ($IV = 0.60$ or $\sqrt{v} = 0.60$). See Appendix C.1 for more details.

Panel A. Truncation of Implied Volatility Surface

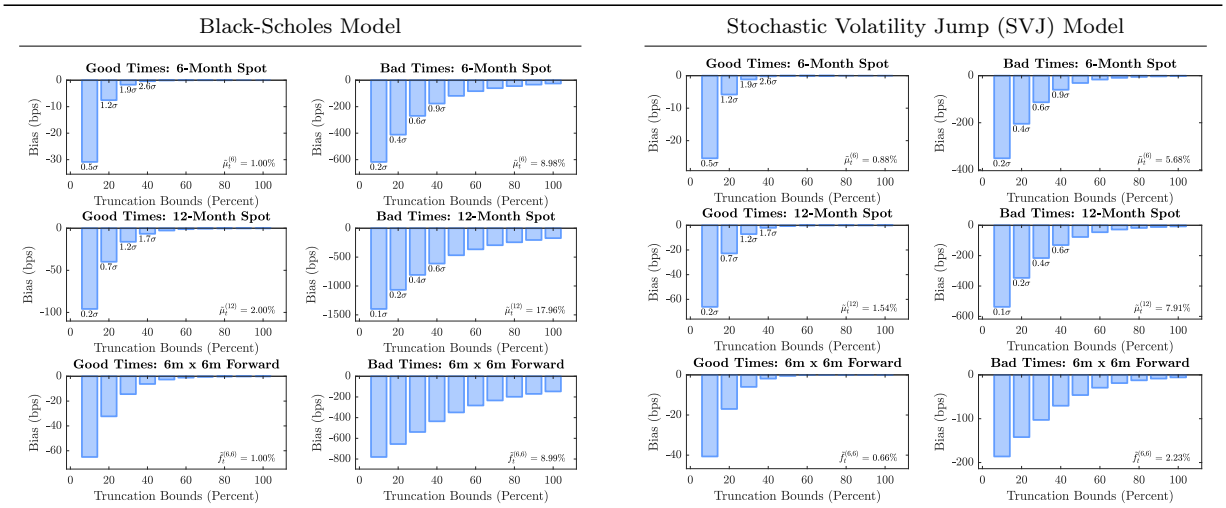

Panel B. Extrapolation of Implied Volatility Surface

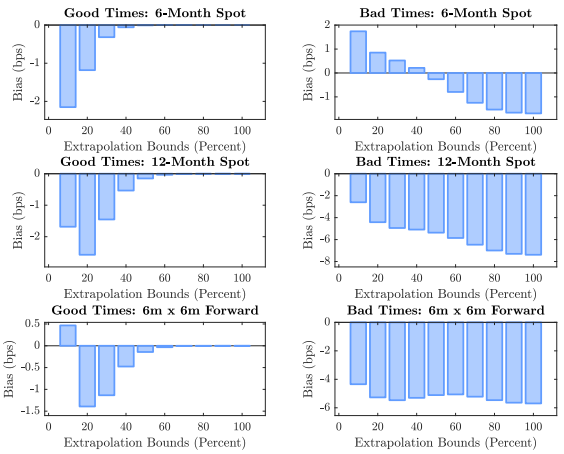

Figure A2
Minimum/Maximum Strike Price: U.S. Sample

This figure plots the minimum/maximum strike price by maturity bin in the U.S. sample. Each bar is the monthly median from daily data. This sample is longest available for each maturity. The black line is the unconditional median from daily data. This sample is the longest available for all maturities. The minimum is the 1st percentile from out-of-the-money put options. The maximum is the 99th percentile from out-of-the-money call options. The units are risk-neutral standard deviations from the forward price: $\frac{K/F-1}{\sigma\sqrt{\tau}}$. See Appendix C.1 for more details.

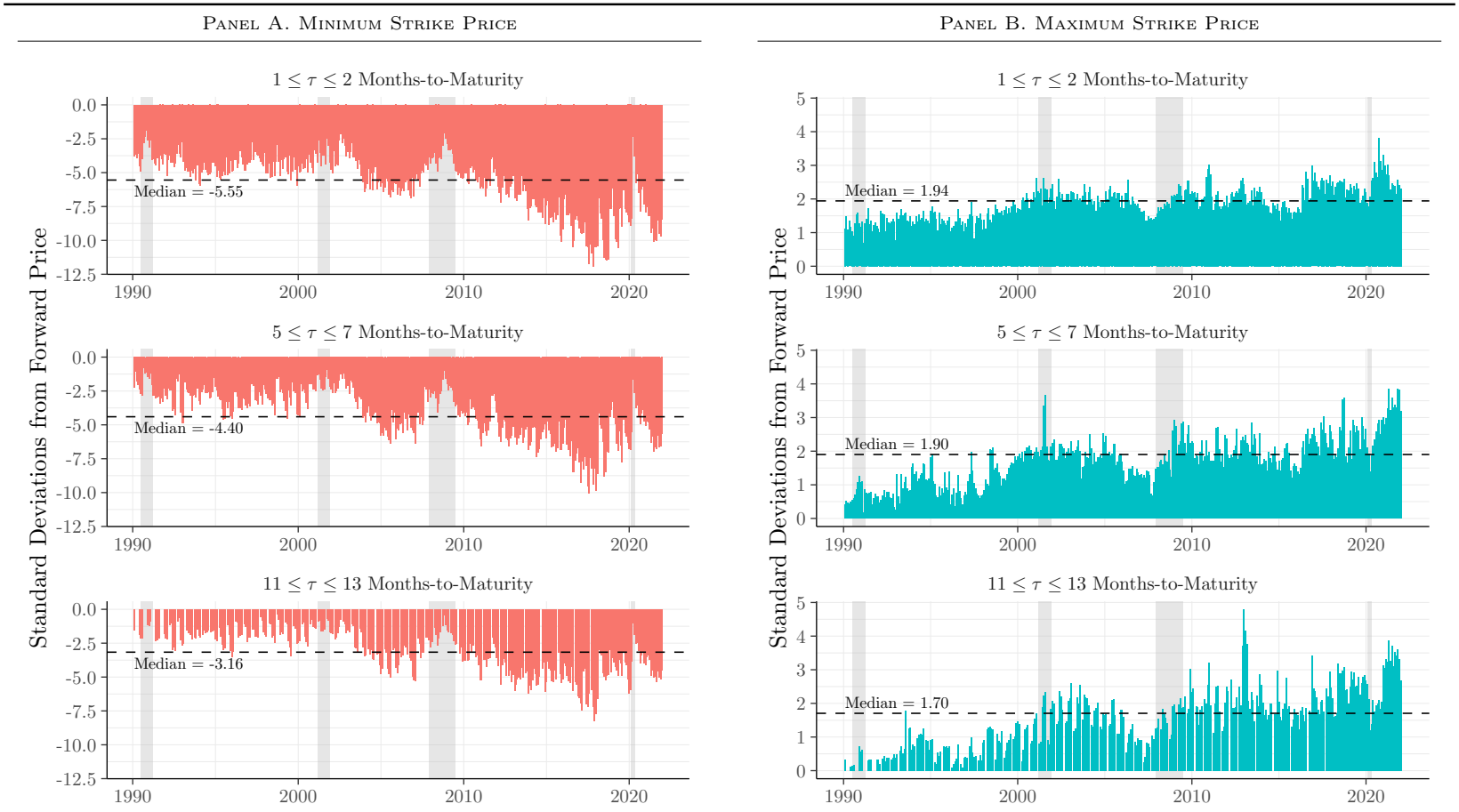

Figure A3
Alternative Integration Bounds

This figure plots 6×6-month forward rates $\tilde{f}_t^{(6,6)}$ (top panel) and the corresponding realized 6-month spot rates $\tilde{\mu}_{t+6}^{(6)}$ (bottom panel) with alternative integration bounds. Spot and forward rates are for option-based risk premia. Gray bands are NBER recessions. The sample is from 01/1990 to 06/2021 in the U.S. See Appendix C.1 for more details.

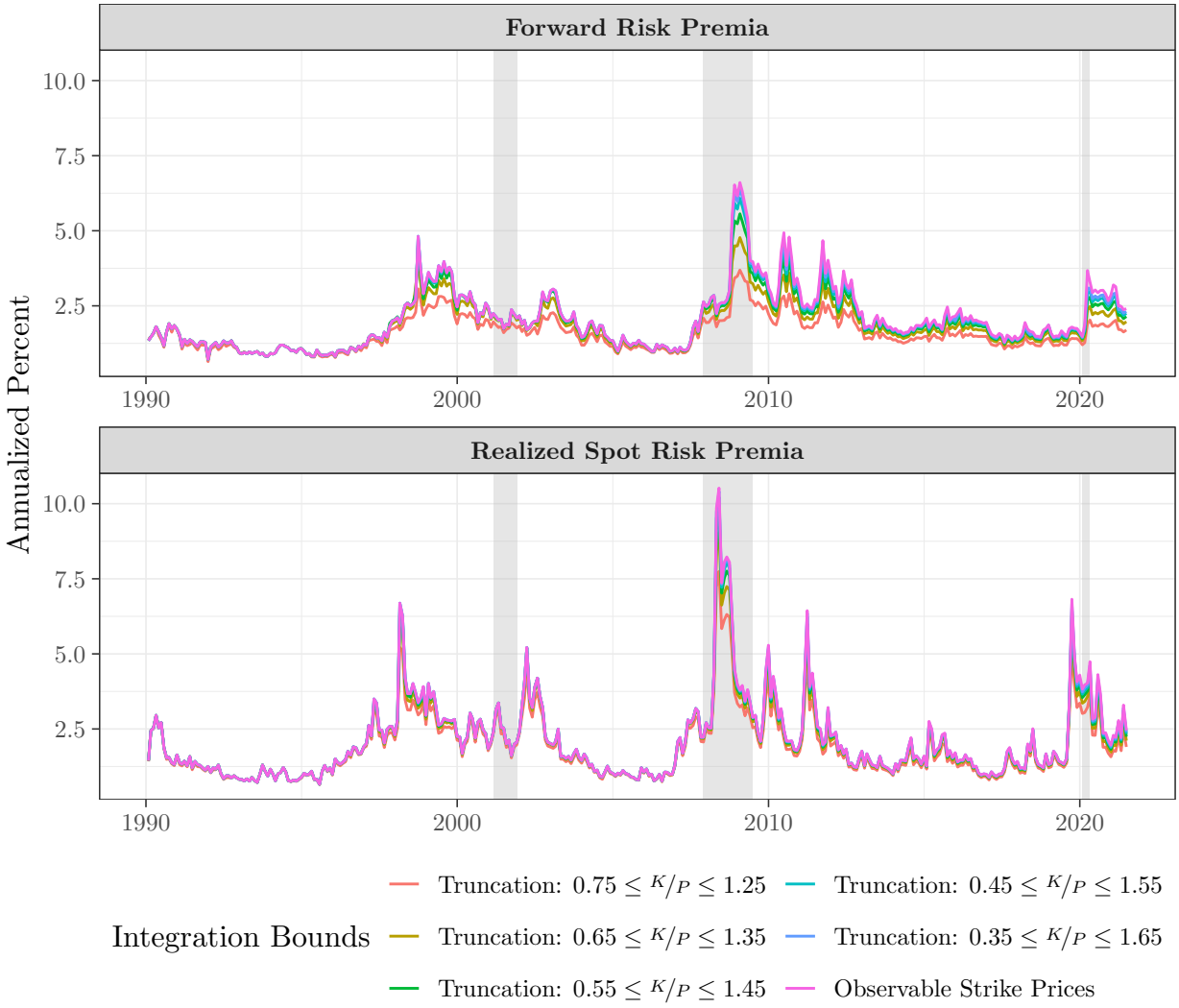

Figure A4
CFO Forward Rates

This figure plots unadjusted 1×9-year forward rates (top panel) and the corresponding break-adjusted series (bottom panel). The break adjustment is from a time-series regression of unadjusted forward rates on an indicator variable that equals 1 on and after 09/2020:

$$\text{unadjusted } \tilde{f}_t^{(1y,9y)} = \beta_0 + \beta_1 \, \mathbb{1}_{t \geq 2020} + e_t$$
$$\text{break-adjusted } \tilde{f}_t^{(1y,9y)} = \text{unadjusted } \tilde{f}_t^{(1y,9y)} - \beta_1 \, \mathbb{1}_{t \geq 2020}.$$

Forward rates are for risk premia. Gray bands are NBER recessions. The sample is quarterly from 12/2001 to 06/2025. See Appendix B.3 for more details.

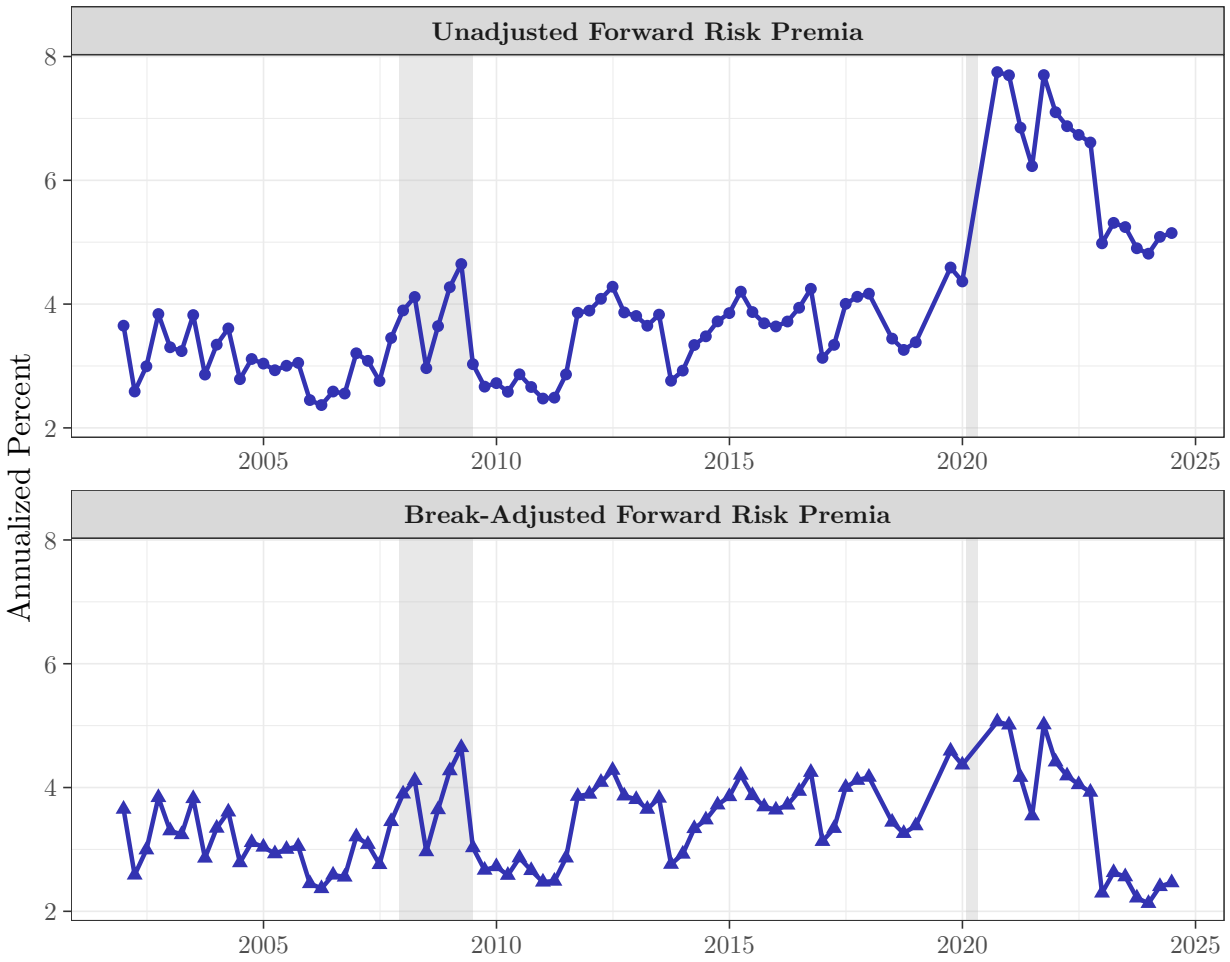

Figure A5
Cyclical Variation in Forward Risk Premia

This figure reports regressions of contemporaneous forward rates on state variables for option-based (first column) and survey-based (second to fourth columns) expectations for risk premia. The bar height reports the slope t-stat, capped at $t = 5.00$. The bar label reports the uncapped t-stat. The dotted line is the 5% critical value for a one-sided test based on a standard normal distribution, $t = 1.645$. On the left-hand side, the option-based horizon is the 6×6-month forward rate, the Livingston horizon is the 6×6-month forward rate, the CFO horizon is the 1×9-year forward rate, and the Vanguard horizon is the 1×9-year forward rate. On the right-hand side, 1/ExCAPE is the excess cyclically-adjusted earnings yield (obtained from Robert Shiller's website), VIX^2 is the squared 1-year CBOE Volatility Index (obtained from the CBOE's website), and NBER is a recession indicator. Each regression reports Newey-West standard errors with $L = \lceil 1.3 \times T^{1/2} \rceil$ lags and fixed-b p-values, following Lazarus et al. (2018). The option-based sample is monthly from 01/1990 to 12/2021. The Livingston sample is half-yearly from 06/1992 to 12/2021. The CFO sample is quarterly from 12/2001 to 06/2025; each regression includes an indicator variable that equals 1 on and after 09/2020. The Vanguard sample is bimonthly from 02/2017 to 12/2024 (including 03/2020). See Section 4.3 for more details.

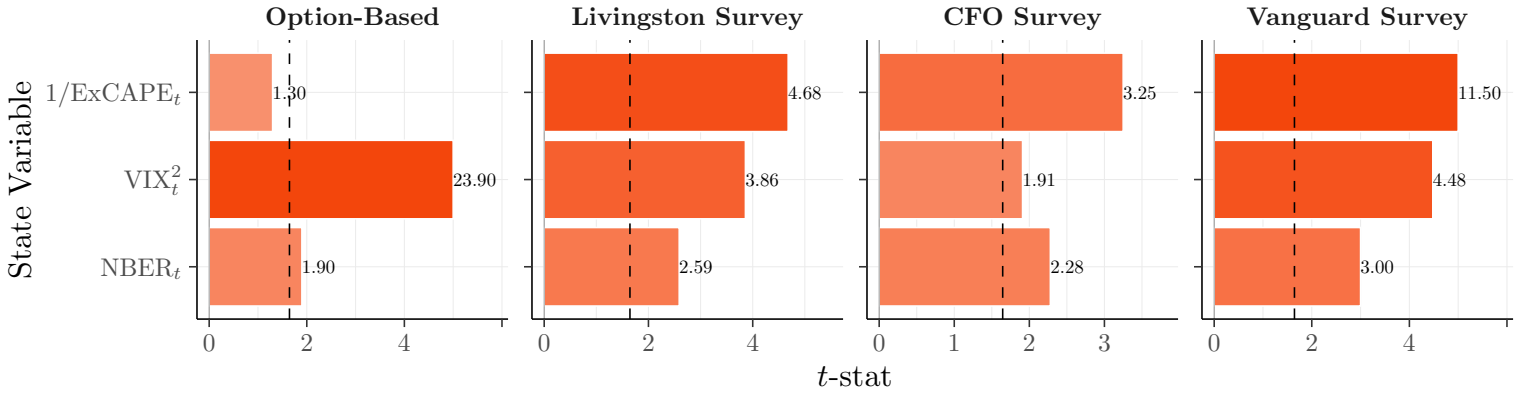

Figure A6
Cyclical Variation in Forward Rates

This figure reports covariances between contemporaneous forward rates and state variables for option-based (first column) and survey-based (second to fourth columns) expectations for risk premia (top row) and expected returns (bottom row). The color reports the sign of the covariance. The horizontal axis reports reports the significance of the covariance: procyclical indicates a significant negative covariance, acyclical indicates a statistically insignificant covariance, and countercyclical indicates a significant positive covariance. On the left-hand side, the option-based horizon is the 6×6-month forward rate, the Livingston horizon is the 6×6-month forward rate, the CFO horizon is the 1×9-year forward rate, and the Vanguard horizon is the 1×9-year forward rate. On the right-hand side, the state variables are the excess CAPE yield for risk premia and CAPE yield for expected returns; the repurchase-adjusted P/D ratio from Nagel and Xu (2022); the P/D and P/E ratio from Welch and Goyal (2008); the 1-year VIX^2; an NBER recession indicator; the risk aversion index from Bekaert, Engstrom, and Xu (2022); the real activity factor from Ludvigson and Ng (2009); the credit spread index from Gilchrist and Zakrajšek (2012), updated by Favara et al. (2016); the Philly Fed Economic Activity Index; the Chicago Fed National Activity Index (CFNAI), National Financial Conditions Index (NFCI), and Adjusted National Financial Conditions Index (ANFCI); the St. Louis Fed Financial Stress Index (STLFSI); the Kansas City Fed Financial Stress Index (KCFSI); and as a summary, the first principal component of the longest available FCI/FSI series (NFCI, ANFCI, and KCFSI). Each state variable is signed such that that higher values correspond to bad times (measured as having a positive covariance with the recession indicator), so positive covariances in the figure indicate countercyclical forward return expectations. Each regression reports Newey-West standard errors with $L = \lceil 1.3 \times T^{1/2} \rceil$ lags and fixed-b p-values, following Lazarus et al. (2018). The option-based sample is monthly from 01/1990 to 12/2021. The Livingston sample is half-yearly from 06/1992 to 12/2021. The CFO sample is quarterly from 12/2001 to 06/2025; each regression includes an indicator variable that equals 1 on and after 09/2020. The Vanguard sample is bimonthly from 02/2017 to 12/2024 (including 03/2020). See Section 4.3 for more details.

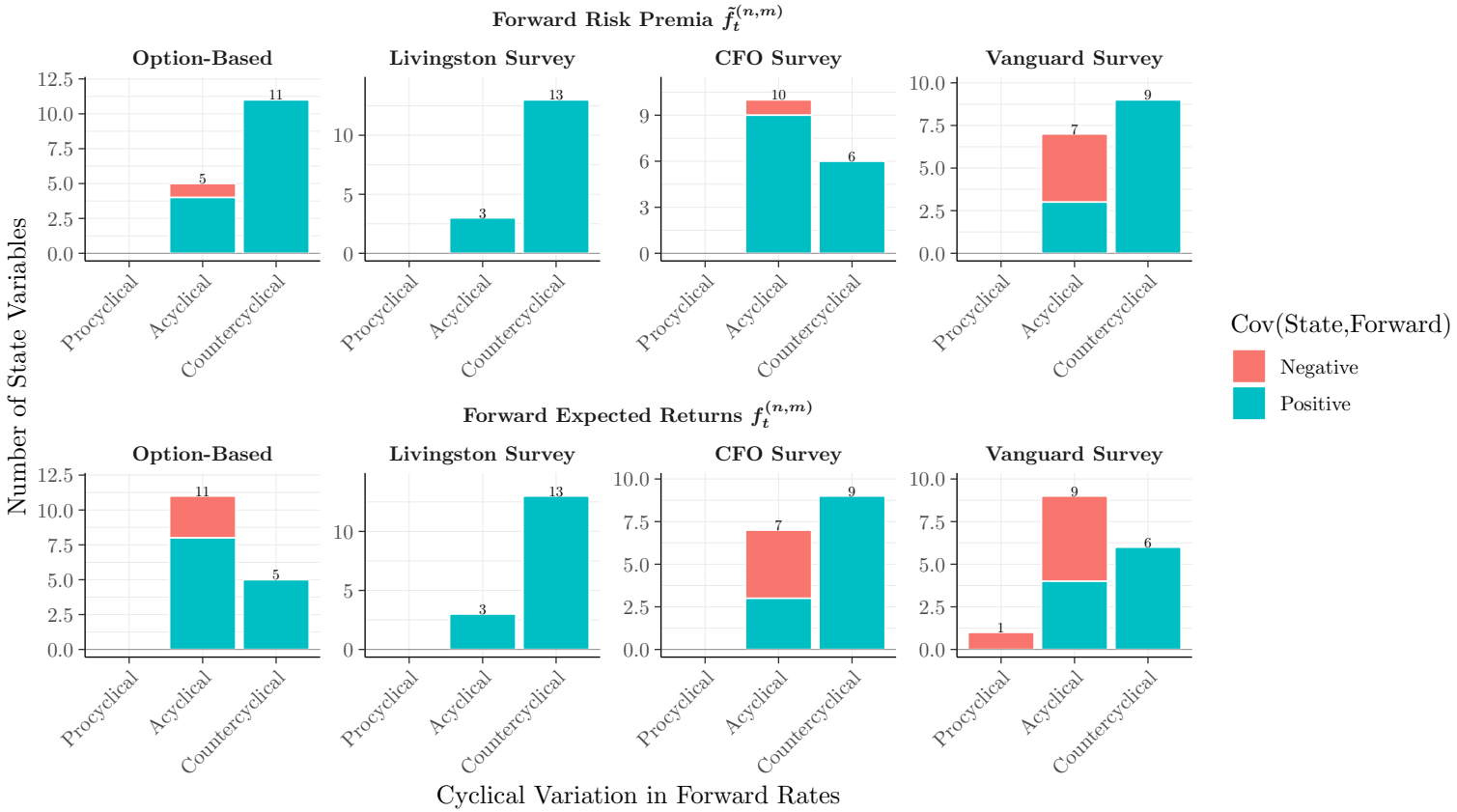

Figure A7
Option-Based Conditional Volatility of the Market Return

This figure plots the conditional volatility of the 6-month market return $\sigma_t(\ln R_{t,t+6})$ from the standpoint of an unconstrained log utility investor fully invested in the market. Gray bands are NBER recessions. The sample is from 01/1990 to 06/2021 in the U.S. See Appendix E.1 for more details.

Figure A8
Model Calibration: Regression Fit

This figure reports estimates in the calibrated model of expectation errors. The model is calibrated with option-based risk premia in the U.S. sample. The black line is the simulated population R^2 in a single long sample with $T = 37,800,000$ months. The gray ribbon is the simulated 95% confidence interval in 100,000 short samples with $T = 378$ months. The red circle is the simulated R^2 under rational expectations with $\theta_F = 0$. The green square is the simulated R^2 under forward rate bias with $\theta_F = 0.0505$. The teal triangle is the observed R^2 in the data with option-based expectations. The purple diamond is the observed R^2 in the data with Livingston survey expectations. The horizon is the 6-month spot rate, 6 months from now. The units are annualized percentage points. Short rate bias $\theta_S = 0$ for all simulated R^2s. See Appendix E.1 for more details.

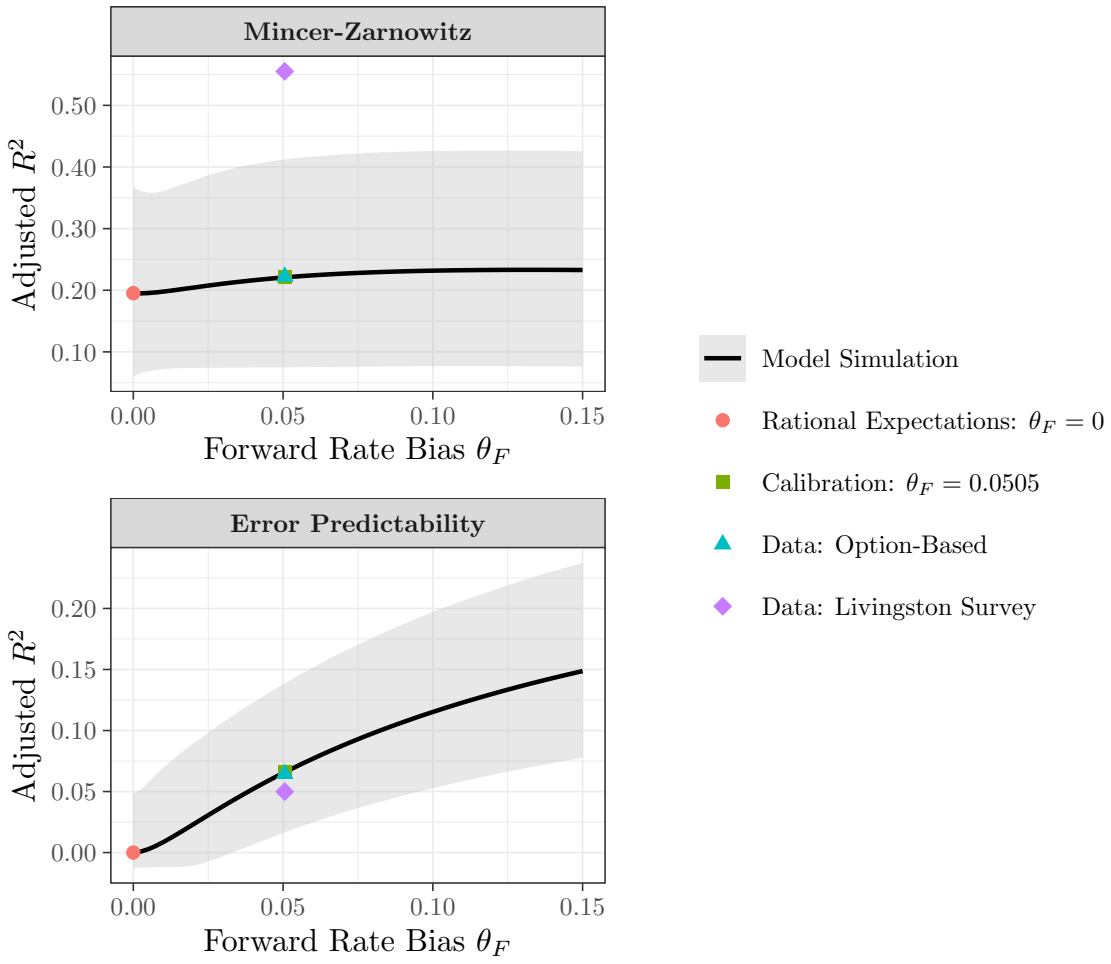

Supplemental Figures

Figure A9
Term Structure of Return Expectations

See Section 2 for more details.

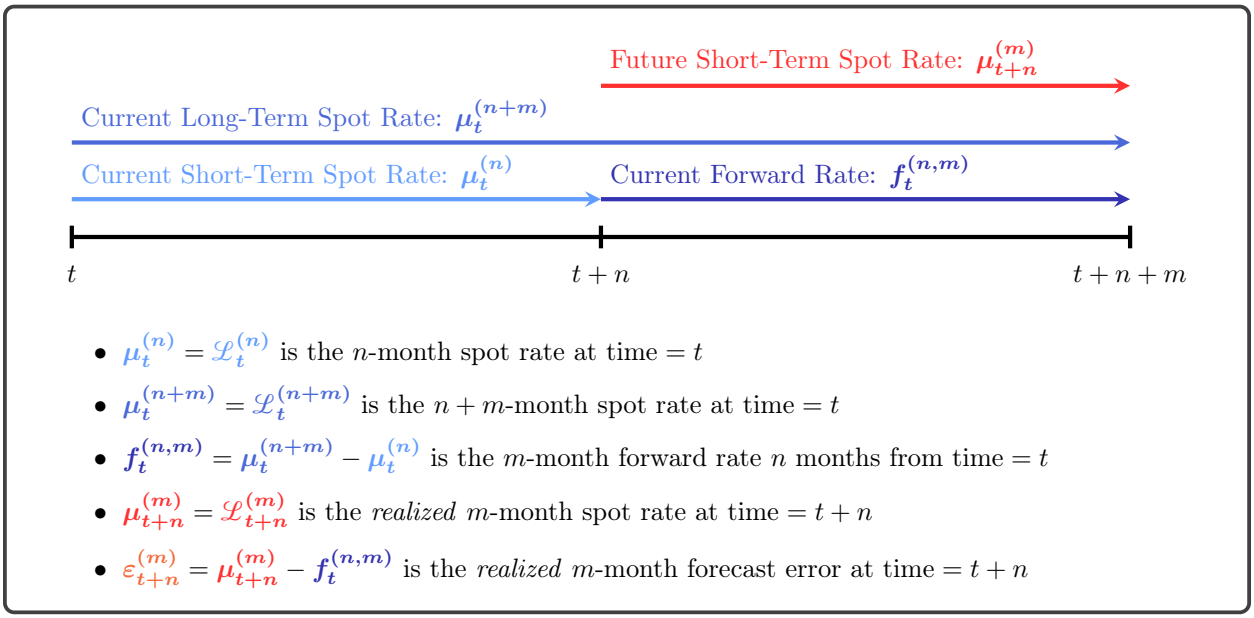

- $\mu_t^{(n)} = \mathcal{L}_t^{(n)}$ is the n-month spot rate at time $= t$
- $\mu_t^{(n+m)} = \mathcal{L}_t^{(n+m)}$ is the $n+m$-month spot rate at time $= t$
- $f_t^{(n,m)} = \mu_t^{(n+m)} - \mu_t^{(n)}$ is the m-month forward rate n months from time $= t$
- $\mu_{t+n}^{(m)} = \mathcal{L}_{t+n}^{(m)}$ is the *realized* m-month spot rate at time $= t+n$
- $\varepsilon_{t+n}^{(m)} = \mu_{t+n}^{(m)} - f_t^{(n,m)}$ is the *realized* m-month forecast error at time $= t+n$

Figure A10
Measuring the LVIX

This figure visualizes the LVIX integral (7) in the Black-Scholes model:

$$\mathcal{L} - r = \frac{1}{P}\int_0^\infty \omega(K) f(K) dK = \frac{1}{P}\left[\int_0^F \frac{\text{put}(K)}{K} dK + \int_F^\infty \frac{\text{call}(K)}{K} dK\right].$$

Time and time-to-maturity dependence are omitted for simplicity. The x-axis units are volatility standard deviations from the forward price: $\frac{K/F-1}{\sigma\sqrt{\tau}}$. Parameters: $P = 100$, $\Delta K = 0.01$, $r = 0.05$, $\tau = 1$, $IV = 0.20$, $q = 0.00$. See Appendix C.1 for more details.

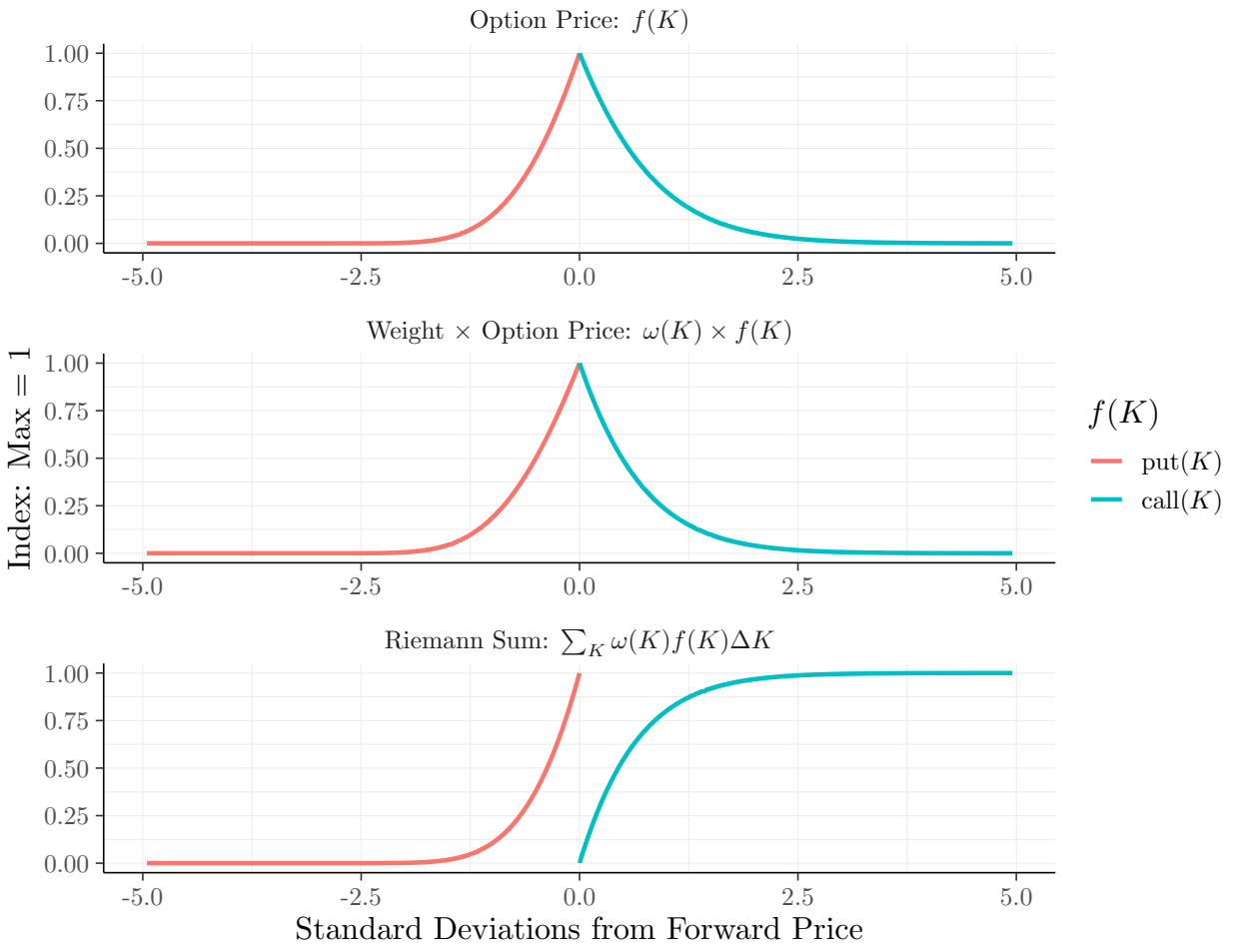

Figure A11
Filtered Option Prices

Panel A plots the number of observations after filters. Panel B plots the share of filtered options with positive open interest. Each bar is the annual median from daily data. This sample is the longest available for each exchange from 1990 to 2020. The black line is the unconditional median from daily data. This sample is from 05/14/2007 to 04/28/2021. Options are out-of-the-money with maturity $7 \leq \tau \leq 365$ days. Belgium, Finland, and the Stoxx Europe 50/600 do not have open interest data. See Appendix B.1 for more details.

Panel A. Number of Observations

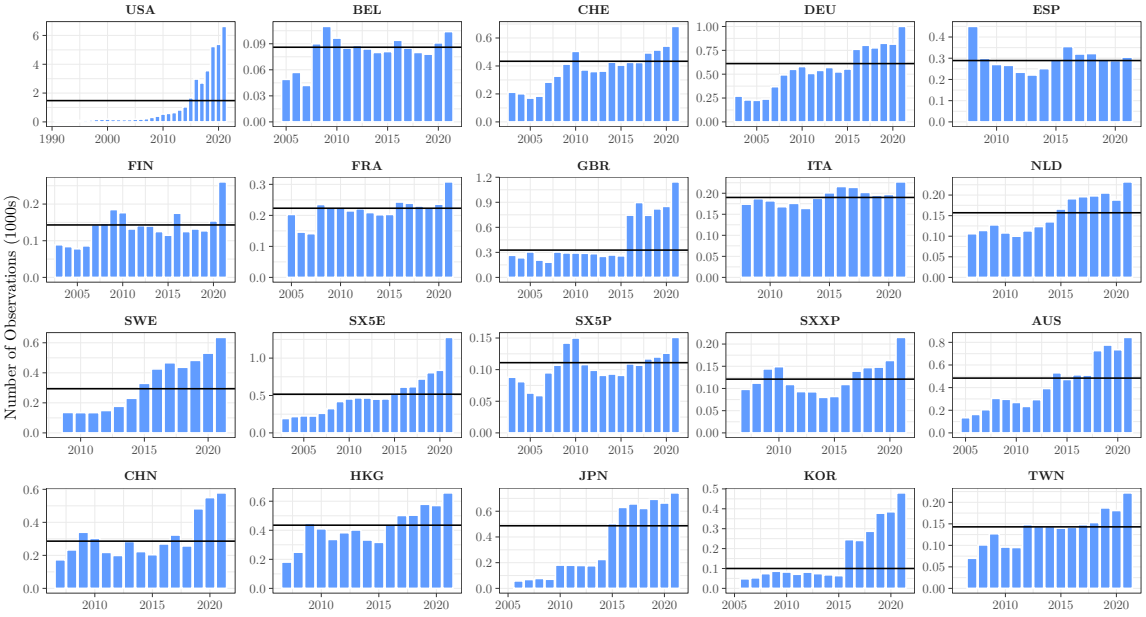

Panel B. Positive Open Interest

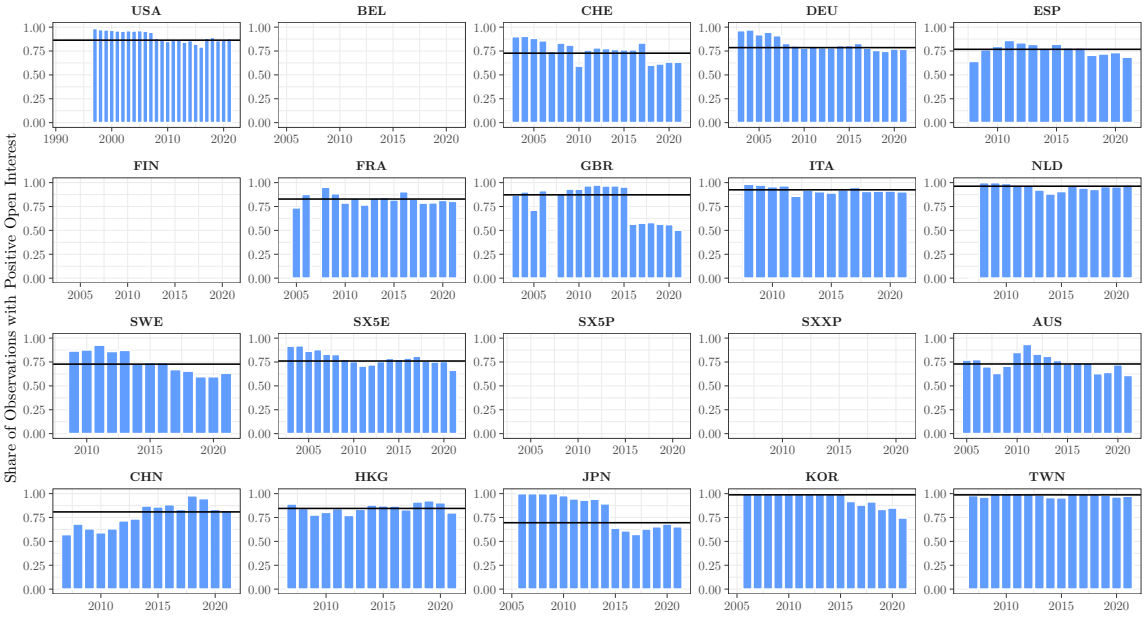

Figure A12
Filtered Option Prices by Maturity

This figure plots the share of filtered options by maturity bin. Each bar is the annual share from daily data. Options are out-of-the-money with maturity $7 \leq \tau \leq 365$ days. The sample is the longest available for each exchange from 1990 to 2020. See Appendix B.1 for more details.

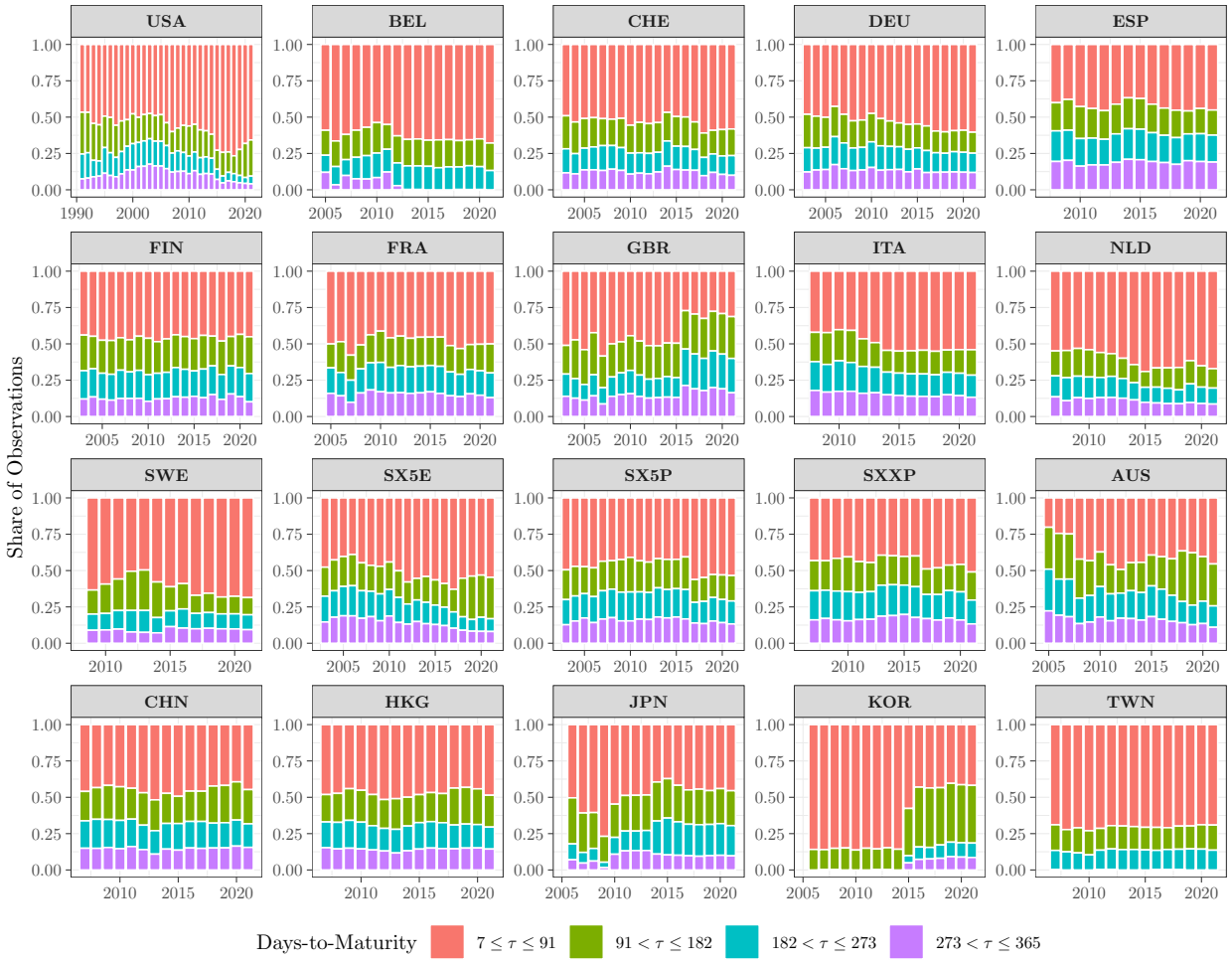

Figure A13
Minimum/Maximum Strike Price: Full Sample

This figure plots the minimum/maximum strike price by maturity bin. The left panel is the annual median from daily data. This sample is the longest available for each exchange from 1990 to 2020. The right panel is the unconditional median from daily data. This sample is from 05/14/2007 to 04/28/2021. The minimum is the 1st percentile from out-of-the-money put options. The maximum is the 99th percentile from out-of-the-money call options. The units are risk-neutral standard deviations from the forward price: $\frac{K/F-1}{\sigma\sqrt{\tau}}$. See Appendix B.1 for more details.

Panel A. Minimum Strike Price: $5 \leq \tau \leq 7$ Months-to-Maturity

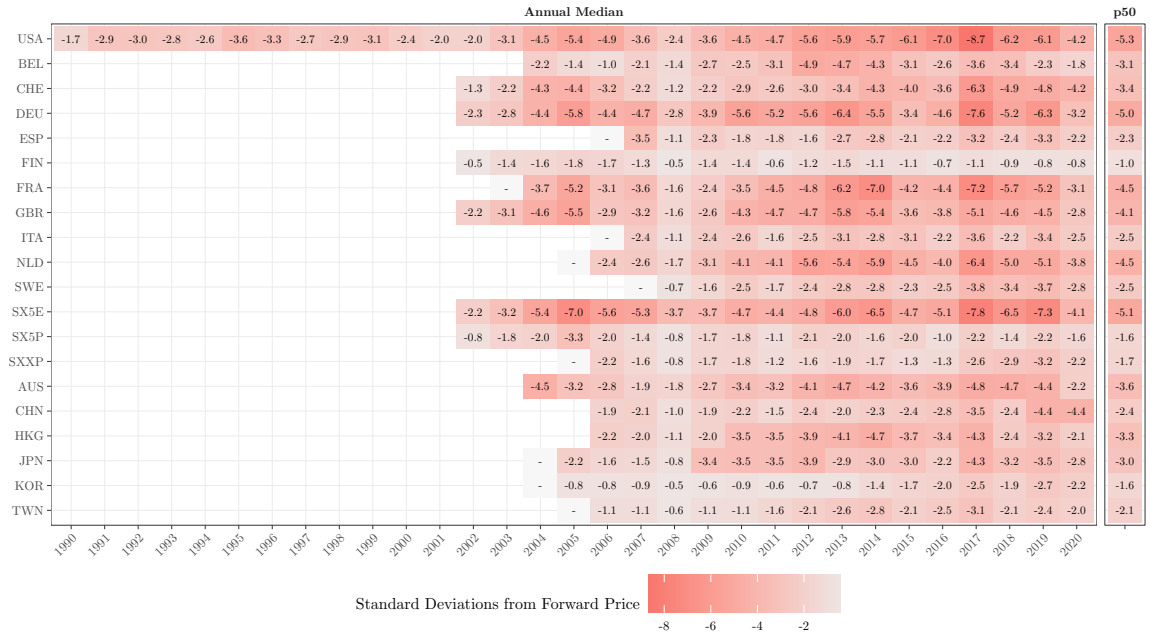

Panel B. Maximum Strike Price: $5 \leq \tau \leq 7$ Months-to-Maturity

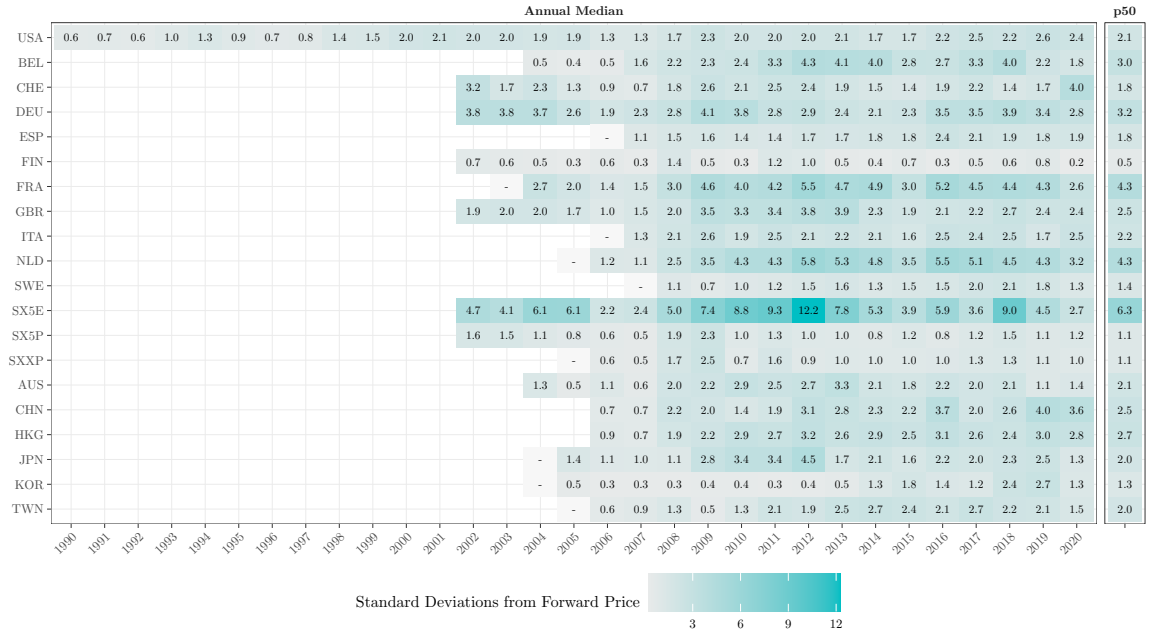

(Continued on the next page)

Figure A13
Minimum/Maximum Strike Price: Full Sample (Continued)

Panel C. Minimum Strike Price: $11 \leq \tau \leq 13$ Months-to-Maturity

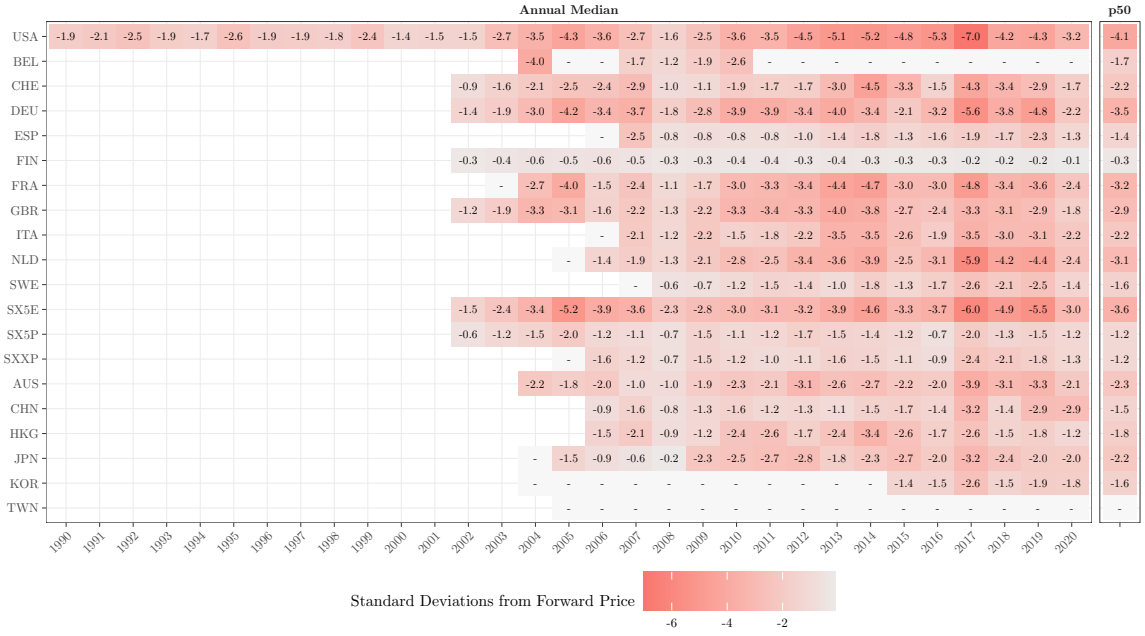

Panel D. Maximum Strike Price: $11 \leq \tau \leq 13$ Months-to-Maturity

(Continued from the previous page)

Figure A14
Surface Triangulation

This figure plots the surface triangulation of option prices on four dates in the U.S. sample. The dots are observed option prices with moneyness $0.80 \leq {}^{K}/_{P} \leq 1.20$ and maturity $30 \leq \tau \leq 365$ days. See Appendix B.2 for more details.

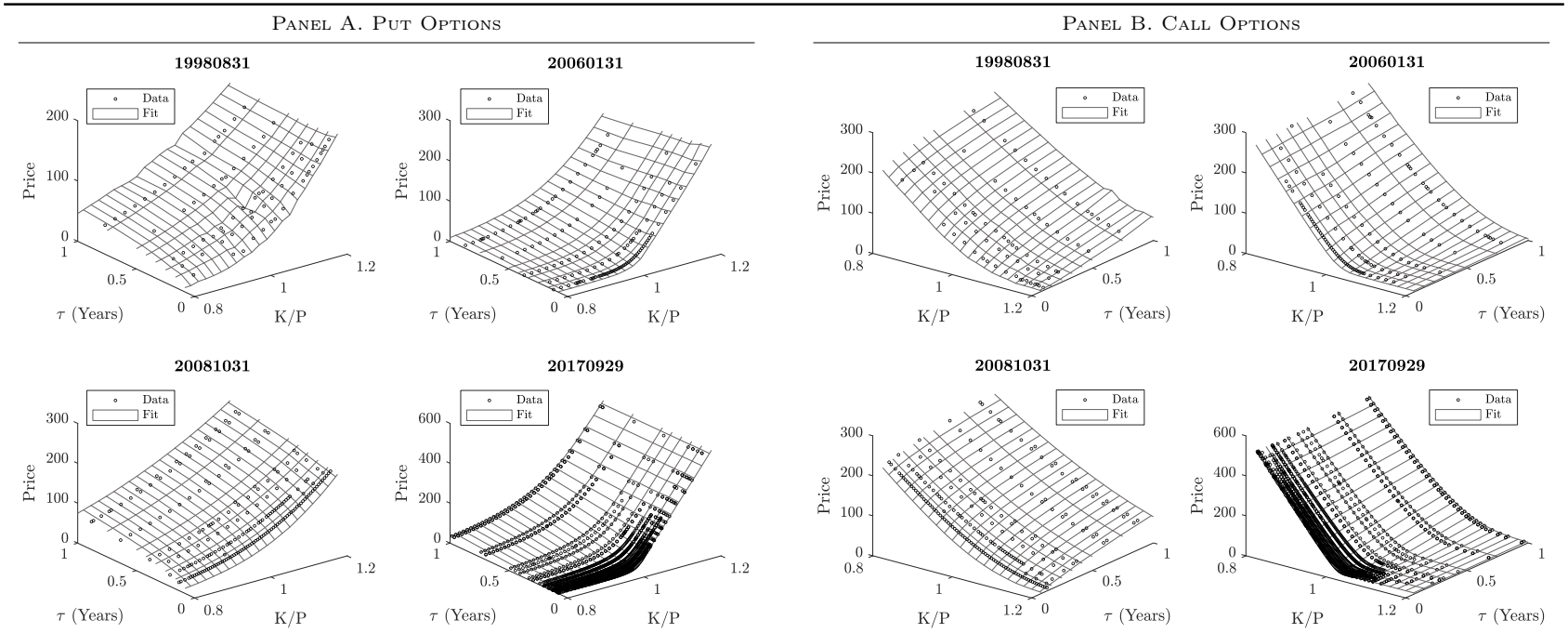

Figure A15
Option-Based Spot and Forward Rates: Full Sample

Panel A plots contemporaneous 6-month spot rates $\tilde{\mu}_t^{(6)}$ (light blue) and 6×6-month forward rates $\tilde{f}_t^{(6,6)}$ (dark blue). Panel B plots instrumented 6×6-month forward rates $\tilde{f}_t^{(6,6)}$ (dark blue) and the corresponding realized 6-month spot rates $\tilde{\mu}_{t+6}^{(6)}$ (red). The instrument is the 2×1-month forward rate: see Table 3 for more details. Spot and forward rates are for option-based risk premia. Gray bands are NBER recessions. The sample is the longest available for each exchange. See Appendix C.3 for more details.

Panel A. Contemporaneous Spot and Forward Risk Premia

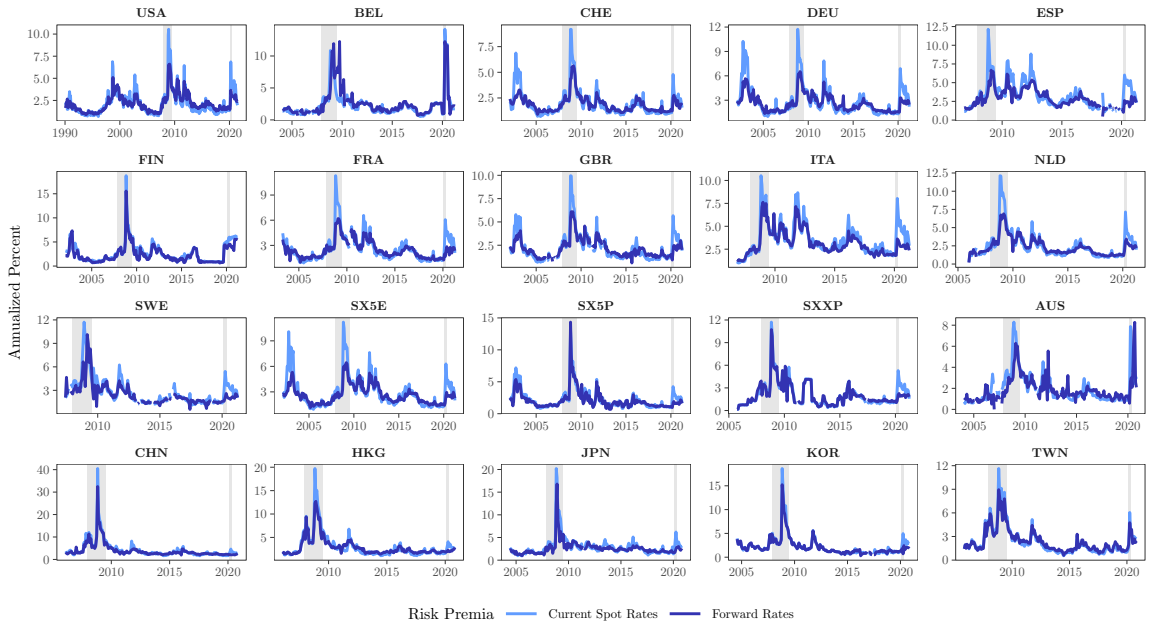

Panel B. Forward and Realized Spot Risk Premia

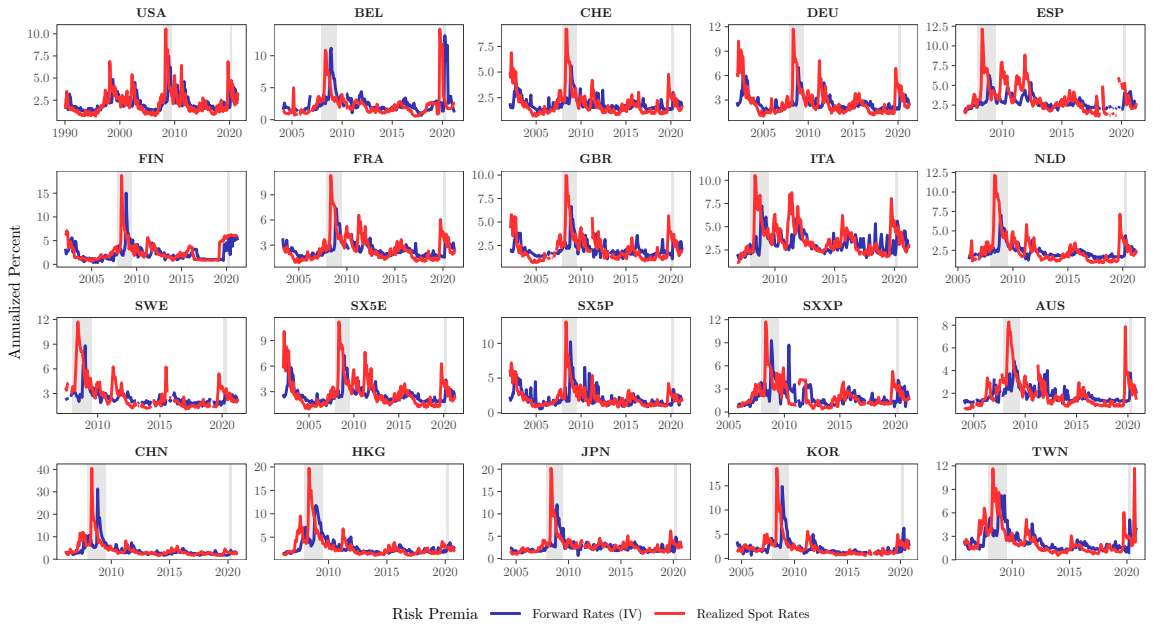

Figure A16
Power Utility: Regression Slopes and Average Forecast Errors

This figure reports estimates from the standpoint of an unconstrained power utility investor fully invested in the market for option-based risk premia. The sample is the longest available for each exchange in the main sample. See Appendix D.1 for more details.

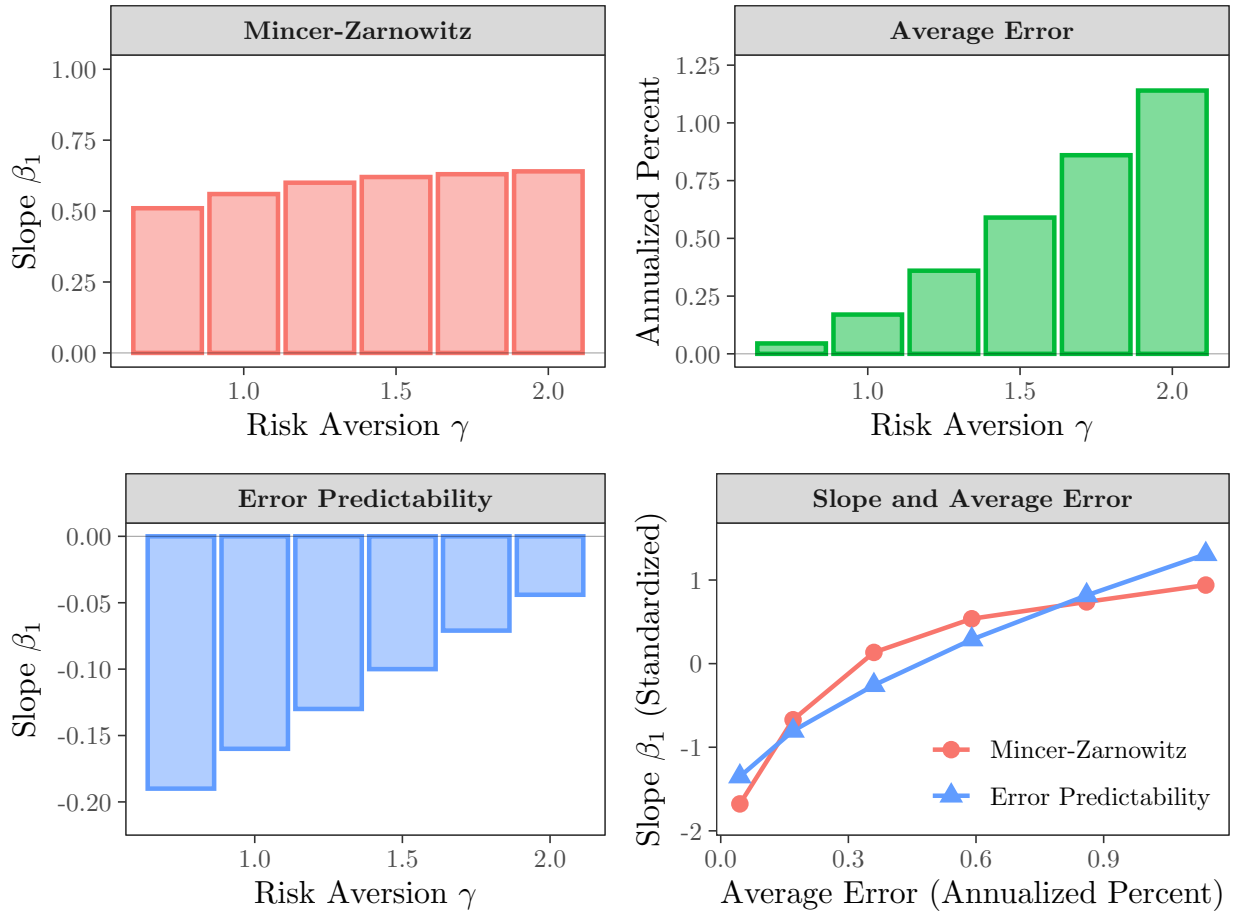

Appendix References

Aït-Sahalia, Yacine and Jefferson Duarte. 2003. "Nonparametric option pricing under shape restrictions." *Journal of Econometrics* 116 (1-2):9–47.

Andersen, Torben G., Oleg Bondarenko, and Maria T. Gonzalez-Perez. 2015. "Exploring Return Dynamics via Corridor Implied Volatility." *Review of Financial Studies* 28 (10):2902–2945.

Bakshi, Gurdip, Charles Cao, and Zhiwu Chen. 1997. "Empirical Performance of Alternative Option Pricing Models." *Journal of Finance* 52 (5):2003–2049.

Bakshi, Gurdip, Nikunj Kapadia, and Dilip Madan. 2003. "Stock Return Characteristics, Skew Laws, and the Differential Pricing of Individual Equity Options." *Review of Financial Studies* 16 (1):101–143.

Barberis, Nicholas, Robin Greenwood, Lawrence Jin, and Andrei Shleifer. 2015. "X-CAPM: An extrapolative capital asset pricing model." *Journal of Financial Economics* 115 (1):1–24.

Bates, David S. 1996. "Jumps and Stochastic Volatility: Exchange Rate Processes Implicit in Deutsche Mark Options." *Review of Financial Studies* 9 (1):69–107.

Beason, Tyler and David Schreindorfer. 2022. "Dissecting the Equity Premium." *Journal of Political Economy* 130 (8):2203–2222.

Bekaert, Geert, Eric C. Engstrom, and Nancy R. Xu. 2022. "The Time Variation in Risk Appetite and Uncertainty." *Management Science* 68 (6):3975–4004.

Berger, David, Ian Dew-Becker, and Stefano Giglio. 2020. "Uncertainty Shocks as Second-Moment News Shocks." *Review of Economic Studies* 87 (1):40–76.

Binsbergen, Jules H. van and Ralph S.J. Koijen. 2017. "The term structure of returns: Facts and theory." *Journal of Financial Economics* 124 (1):1–21.

Black, Fischer and Myron Scholes. 1973. "The Pricing of Options and Corporate Liabilities." *Journal of Political Economy* 81 (3):637–654.

Breeden, Douglas T. and Robert H. Litzenberger. 1978. "Prices of State-Contingent Claims Implicit in Option Prices." *Journal of Business* 51 (4):621–651.

Campbell, John Y. 2017. "Discussion of Lawrence Jin and Pengfei Sui, 'Asset Pricing with Return Extrapolation'." NBER Behavioral Finance Meeting.

Campbell, John Y. and Robert J. Shiller. 1988. "The Dividend-Price Ratio and Expectations of Future Dividends and Discount Factors." *Review of Financial Studies* 1 (3):195–228.

Carr, Peter and Dilip Madan. 1998. "Towards a Theory of Volatility Trading." In *Volatility: New Estimation Techniques for Pricing Derivatives*. Cambridge University Press, 417–427.

Constantinides, George M., Jens Carsten Jackwerth, and Alexi Savov. 2013. "The Puzzle of Index Option Returns." *Review of Asset Pricing Studies* 3 (2):229–257.

Culp, Christopher L., Yoshio Nozawa, and Pietro Veronesi. 2018. "Option-Based Credit Spreads." *American Economic Review* 108 (2):454–88.

De la O, Ricardo and Sean Myers. 2021. "Subjective Cash Flow and Discount Rate Expectations." *Journal of Finance* 76 (3):1339–1387.

Dew-Becker, Ian and Stefano Giglio. 2023. "Cross-Sectional Uncertainty and the Business Cycle: Evidence from 40 Years of Options Data." *American Economic Journal: Macroeconomics* 15 (2):65–96.

Duarte, Jefferson, Christopher S. Jones, and Junbo L. Wang. 2024. "Very Noisy Option Prices and Inference Regarding the Volatility Risk Premium." *Journal of Finance* 79 (5):3581–3621.

Favara, Giovanni, Simon Gilchrist, Kurt F. Lewis, and Egon Zakrajšek. 2016. "Updating the Recession Risk and the Excess Bond Premium." FEDS Notes, Board of Governors of the Federal Reserve System.

Figlewski, Stephen. 2010. "Estimating the Implied Risk-Neutral Density for the US Market Portfolio." In *Volatility and Time Series Econometrics: Essays in Honor of Robert Engle*, edited by Tim Bollerslev, Jeffrey Russell, and Mark Watson. Oxford University Press, 323–353.

Gao, Can and Ian W.R. Martin. 2021. "Volatility, Valuation Ratios, and Bubbles: An Empirical Measure of Market Sentiment." *Journal of Finance* 76 (6):3211–3254.

Gatheral, Jim. 2011. *The Volatility Surface: A Practitioner's Guide*. John Wiley & Sons.

Gatheral, Jim and Antoine Jacquier. 2011. "Convergence of Heston to SVI." *Quantitative Finance* 11 (8):1129–1132.

———. 2014. "Arbitrage-Free SVI Volatility Surfaces." *Quantitative Finance* 14 (1):59–71.

Gilchrist, Simon and Egon Zakrajšek. 2012. "Credit Spreads and Business Cycle Fluctuations." *American Economic Review* 102 (4):1692–1720.

Gormsen, Niels Joachim and Christian Skov Jensen. 2025. "Higher-Moment Risk." *Journal of Finance* Forthcoming.

Graham, John, Brent Meyer, Nicholas Parker, and Sonya Ravindranath Waddell. 2020. "Introducing The CFO Survey: A collaboration between Duke University's Fuqua School of Business and the Federal Reserve Banks of Richmond and Atlanta." URL https://www.richmondfed.org/research/national_economy/cfo_survey/research_and_commentary/2020/20200515_introducing_cfo_survey.

Jiang, George J. and Yisong S. Tian. 2007. "Extracting Model-Free Volatility from Option Prices: An Examination of the VIX Index." *Journal of Derivatives* 14 (3):35–60.

Kelly, Bryan, Hanno Lustig, and Stijn Van Nieuwerburgh. 2016. "Too-Systemic-to-Fail: What Option Markets Imply about Sector-Wide Government Guarantees." *American Economic Review* 106 (6):1278–1319.

Kelly, Bryan, Ľuboš Pástor, and Pietro Veronesi. 2016. "The Price of Political Uncertainty: Theory and Evidence from the Option Market." *Journal of Finance* 71 (5):2417–2480.

Lazarus, Eben, Daniel J. Lewis, James H. Stock, and Mark W. Watson. 2018. "HAR Inference: Recommendations for Practice." *Journal of Business & Economic Statistics* 36 (4):541–559.

Ludvigson, Sydney C. and Serena Ng. 2009. "Macro Factors in Bond Risk Premia." *Review of Financial Studies* 22 (12):5027–5067.

Malz, Allan M. 2014. "A Simple and Reliable Way to Compute Option-Based Risk-Neutral Distributions." Staff Report 677, Federal Reserve Bank of New York.

Martin, Ian. 2017. "What is the Expected Return on the Market?" *Quarterly Journal of Economics* 132 (1):367–433.

Martin, Ian W.R. and Christian Wagner. 2019. "What is the Expected Return on a Stock?" *Journal of Finance* 74 (4):1887–1929.

Mincer, Jacob A. and Victor Zarnowitz. 1969. "The Evaluation of Economic Forecasts." In *Economic Forecasts and Expectations*. National Bureau of Economic Research, 3–46.

Nagel, Stefan and Zhengyang Xu. 2022. "Asset Pricing with Fading Memory." *Review of Financial Studies* 35 (5):2190–2245.

Newey, Whitney K. and Kenneth D. West. 1987. "A Simple, Positive Semi-Definite, Heteroskedasticity and Autocorrelation Consistent Covariance Matrix." *Econometrica* 55 (3):703–708.

Welch, Ivo and Amit Goyal. 2008. "A Comprehensive Look at the Empirical Performance of Equity Premium Prediction." *Review of Financial Studies* 21 (4):1455–1508.